


 Received 24th June 2014  
 Accepted 7th October 2014

 DOI: 10.1039/c4ra11444b  
[www.rsc.org/advances](http://www.rsc.org/advances)

## ortho-Quinone methide (o-QM): a highly reactive, ephemeral and versatile intermediate in organic synthesis

Maya Shankar Singh,\* Anugula Nagaraju, Namrata Anand and Sushobhan Chowdhury

Since its first observation in 1907, *ortho*-quinone methide (o-QM) has occupied a strategic place within the framework of reactive intermediates in organic synthesis. In recent years, o-QM has enhanced its importance as a versatile reactive intermediate, and its applications in organic synthesis, material chemistry, fine chemicals, and pharmaceuticals are increasing rapidly. This critical review summarizes the key concepts behind o-QMs and provides an overview of current applications in organic synthesis to provide an appropriate background for synthetic, medicinal and combinatorial developments. This review covers the literature from its origin to the mid of 2014 (112 references).

### 1. Introduction

*Department of Chemistry, Faculty of Science, Banaras Hindu University, Varanasi 221 005, India. E-mail: mssingh@bhu@yahoo.co.in; Fax: +91-542-2368127; Tel: +91-542-6702502*



Maya Shankar Singh born in 1960, received his MSc degree in Organic Chemistry from Banaras Hindu University, Varanasi, India in 1981, where he also earned his PhD degree in 1986 working under the tutelage of Professor K. N. Mehrotra. After his postdoctoral work, he joined Vikram University Ujjain in 1990 as Assistant Professor in Organic Chemistry, and moved to Gorakhpur University as Associate Professor in 1998,

then to Banaras Hindu University in 2004, where he is currently Professor in Organic Chemistry since 2006. During his sabbatical, he visited the Chemistry Department of the University of Arizona, Tucson, USA; Nagoya Institute of Technology, Nagoya, Japan; Loughborough University, UK and University of Leicester, UK. His research interests are centered on synthetic Organic chemistry with special emphasis in the development of novel building block precursors, new eco-compatible synthetic methods, multicomponent domino/tandem reactions, and structural studies. Fifteen students have completed their PhD degrees under his supervision. He has published 125 research articles and four reviews in journals of high status. Additionally, Prof. Singh has also authored three textbooks in organic chemistry published from Pearson-Education and Wiley-VCH, Weinheim, Germany. He has been elected as a fellow of the Indian Academy of Sciences, India in 2013.



Anugula Nagaraju was born in Chandurthi, Karimnagar, Andhra Pradesh, India, in 1986. He received his BSc and MSc degrees in Chemistry from Kakatiya University, Warangal in 2007 and 2010, respectively. Currently, he is pursuing his Ph.D. under the supervision of Professor Maya Shankar Singh at Banaras Hindu University, Varanasi, India. His major research interest is to develop new synthetic methodologies and novel reagents for the synthesis of bioactive molecules.

chemistry, fine chemicals, and pharmaceuticals.<sup>1</sup> The *ortho*-quinone methide (*o*-QM) was first suggested by Fries in 1907 and is generally formed by the reaction of phenol with aldehyde in the presence of an acid or a base. The first direct evidence was given by Gardner in 1963 by trapping it at  $-100\text{ }^{\circ}\text{C}$ . After 1963, its use as a versatile intermediate in organic synthesis increased enormously, particularly in many tandem [4 + 2] cycloaddition reactions with a variety of dienophiles. However, there are abundant indirect evidences for the *in situ* generation of *ortho*-quinone methides. Most indirect evidence comes from the structural identification of the products that result from dimerization, trimerization, intramolecular and intermolecular [2 + 2] cycloadditions as well as the nucleophilic trapping of *o*-QMs.<sup>2</sup> The chemical behaviour of *o*-QMs resembles that of  $\alpha$ ,  $\beta$ -unsaturated ketones due to the presence of a 1,3-cyclohexadiene core substituted with a carbonyl and an exo-methylene group. They react very rapidly with nucleophiles and undergo efficient Diels–Alder reactions with electron-rich olefins. Expansive reactivity of the *o*-QM can be used in the linchpin reaction for the construction of various natural products.<sup>3</sup>

Compared to carbocations, carbanions, radicals, carbenes, nitrenes and so forth, *ortho*-quinone methides are relative newcomers to the family of inherently reactive species. Quinone methides exist in three isomeric forms *o*-, *m*-, and *p*-quinone methides (also known as *o*-, *m*-, and *p*-QMs) (Fig. 1). *meta*-Quinone methide is actually a resonance hybrid of two canonical forms, one of which is a zwitterionic form stabilized by aromatic conjugation, increasing its polarity and thus enhancing its reactivity. The importance of *o*- and *p*-quinone methides in organic synthesis and their role in biochemistry have been studied in detail. Unlike benzoquinones, *o*- and *p*-quinone methide derivatives are highly polarized compounds, usually observed with difficulty or postulated as reactive intermediates because of the facile reactions driven by the formation of aromatized phenol derivatives.

*ortho*-Quinone methides are highly versatile intermediates that have been extensively harnessed by nature (Fig. 2). A variety

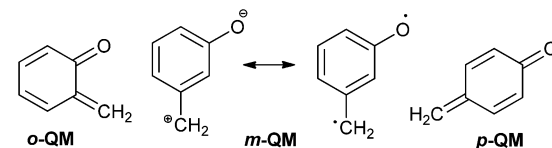


Fig. 1 Isomeric forms of quinone methides.

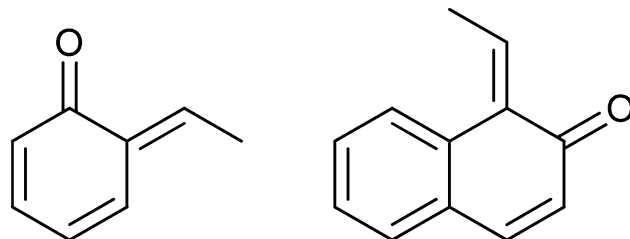


Fig. 2 *ortho*-Quinone methides.

of plants, animals, and insects capitalize upon these types of compounds as a mean of defence. However, despite general knowledge of *o*-QMs for over a century, these intermediates still lie outside the synthetic mainstream. Pettus and Water<sup>1a</sup> reviewed *o*-QMs, particularly its preparation, the benefits and limitations associated with each method as well as the applications in total synthesis.

*ortho*-Quinone methide exists in *E/Z* geometric isomers that are fluxional in nature, and behaves as a combination of a charged zwitterionic and biradical structures (Fig. 3). The distribution among these geometric isomers is believed to result from the differences between non-bonded interactions. If from a steric point of view, R<sup>1</sup> substituent is smaller than oxygen, then the *E*-configuration is preferred. However, increasing the size of R<sup>1</sup> substituent can cause the *Z*-configuration to predominate. The *E/Z* ratio proves important in governing the diastereoselective outcome for Diels–Alder cycloadditions.

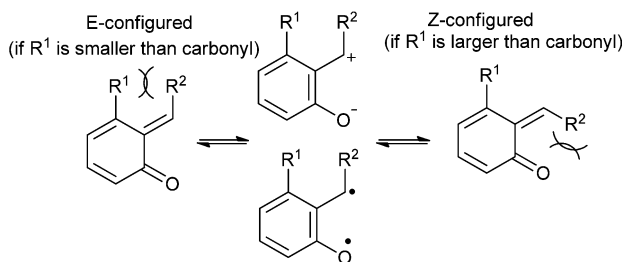


Namrata Anand obtained her BSc (2005) and MSc (2007) degrees in Organic Chemistry from Deen Dayal Upadhyay Gorakhpur University, Gorakhpur (India). In 2013, she completed her Ph.D. at the Central Drug Research Institute, Lucknow (India) with Dr R. P. Tripathi. Since 2013, she is a Postdoctoral Researcher at Banaras Hindu University, Varanasi (India) with Prof. M.S.

Singh. Her current research interests focus on the carbohydrate chemistry and the development of transition-metal catalysed C–H bond activation.



Sushobhan Chowdhury was born in South 24 Parganas, West Bengal, India, in 1985. He received his B. Sc. degree from the University of Calcutta in 2007 and moved to the Banaras Hindu University, Varanasi for post-graduate studies. There he obtained his M. Sc. degree in 2010 and completed Ph.D. under the supervision of Prof. Maya Shankar Singh in 2014. His doctoral study was mainly themed on the development of synthetic methods based on the dithioester chemistry. Presently, he is working as a postdoctoral fellow at UNIST, Ulsan, South Korea.

Fig. 3 Geometric, zwitterionic and biradical structures of *o*-QM.

Quinone methides (QMs) are common reactive intermediates in chemistry, as well as in the photochemistry of phenols, attracting considerable attention recently owing to their biological activity.<sup>4</sup> Although the partial zwitterionic character of QMs makes them both electrophilic and nucleophilic, their reactivity with nucleophiles is particularly important in biological systems. It has been demonstrated that QMs react with amino acids<sup>5</sup> and proteins,<sup>6</sup> and inhibit the action of some enzymes. Moreover, they have been implicated as the ultimate cytotoxins responsible for the function of agents such as anti-tumor drugs, antibiotics, and DNA alkylators in biological chemistry.<sup>7,8</sup> Later on, it was shown that QMs are not the responsible reagents for cross-linking DNA, but they are probably involved in the metabolic formation of formaldehyde.<sup>9</sup> To understand the chemistry of anthracycline antitumor antibiotic, a simple stable *o*-QM has been constructed and entirely characterized. Reaction of quinone methide with nucleophiles, including 2',3'-isopropylideneadenosine has been examined.<sup>10</sup>

Several important clinical drugs like cisplatin, psoralens, and mitomycin C are known to induce DNA ISC (interstrand cross-links) formation, which can disrupt cell maintenance and replication.<sup>11</sup> Both reductive and oxidative metabolisms form quinone methides and have become a very important topic in drug design and drug safety. Even though *ortho*-quinone methides were investigated in detail 50 years ago, the last few years have brought about a renaissance in their chemistry. This review summarizes the recent developments in this field and highlights key historical contributions.

## 2. Generation of *ortho*-quinone methides

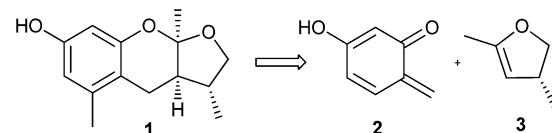
*ortho*-Quinone methides are highly reactive species that have attracted considerable attention because of their intriguing structure and properties. A number of methods for the generation of *o*-QMs have been developed till date, enabling the straightforward construction of diverse aromatic molecules with successful applications to a number of complete syntheses of complex natural products. In the past decade, the most popular methods were photochemical initiation of *o*-( $\alpha$ -phenyl) substituted phenols or thermal initiation of various substituents on the benzene ring of *ortho*-methyleneacetoxy phenols. Lewis acid, base, and chemical oxidants were also used to generate

*o*-QMs. Thus, the method of generation of the *o*-QM becomes intimately linked with the manner in which it is to be utilized.

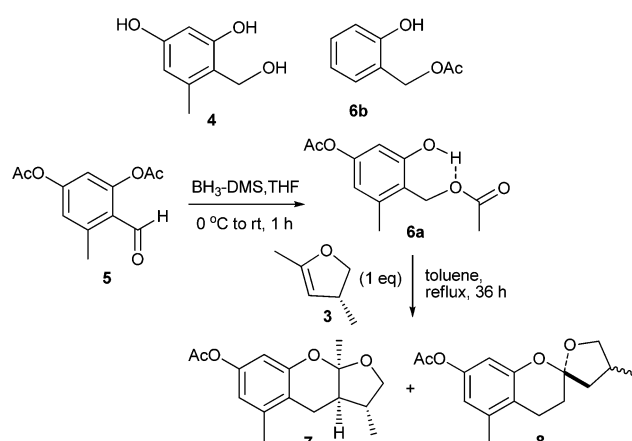
### 2.1. Thermal generation

Among the used procedures to generate *o*-QMs, the most common ones are thermal and base initiations, in which good to excellent stereoselectivity with excellent yields of the corresponding products have been obtained. Only a limited number of accounts have been reported where acid is used to generate the *o*-QMs. This is mainly due to the low compatibility of acid with the dienophiles, and because of the greater ionic character of the reaction conditions that result in a product with low stereoselectivity. Baldwin and co-workers<sup>12</sup> introduced an efficient method for the generation of *o*-QM from *ortho*-methyleneacetoxy phenols that was used for the biomimetic synthesis of ( $\pm$ )-alboatrin (Scheme 1). Alboatrin **1** is a phytotoxic natural product, and its biosynthesis has been realized through hetero Diels–Alder reaction of an orcinol derived *o*-quinone methide **2** and (*R*)-4,5-dihydro-2,4-dimethylfuran **3**.

Baldwin assumed that dehydration of the corresponding hydroxymethyl orcinol derivative **4** would give *o*-QM. Compound **4** was obtained by the reduction of precursor **6b**, which was found to be unstable and rapidly decomposed under the reaction conditions. Then a diacetate **5** was prepared, which was reduced to its alcohol and consequently underwent transesterification by itself to give an *ortho*-methyleneacetoxy phenol **6a** under thermal conditions (Scheme 2). Subsequently, simple heating of **6a** in the presence of dimethylfuran **3** afforded acetylalboatrin **7** as the major product (63%), acetyl *epi*-alboatrin (5%), and an inseparable mixture of diastereoisomers **8** (25%). Deacetylation of **7** yielded the desired ( $\pm$ )-alboatrin, for which



Scheme 1 Retrosynthesis of Alboatrin.

Scheme 2 Synthesis of acetylated ( $\pm$ )-alboatrin (7).

spectral data was found to be identical to the natural ( $\pm$ )-alboatin. Intramolecular hydrogen bonding might facilitate the elimination of acetic acid upon heating through a six-member transition state, furnishing the *o*-quinone methide.

Christopher D. Bray<sup>13</sup> reported the generation of *o*-QM from deprotonation of *ortho*-hydroxybenzyl acetate **9** with *i*PrMgCl under mild anionic reaction conditions, which reacts with *exo*-enol ethers **10** as  $2\pi$  partners in hetero Diels–Alder (HDA) reactions, furnishing *mono*-benzannelated spiroketals **11** (Scheme 3). This rapid and simple strategy is clearly applicable to the synthesis of a wide range of natural products, including berkelic acid, chaetoquadrin A and cephalostatin.

Rosellon and co-workers<sup>14</sup> developed a method for the generation of *ortho*-quinone methides **13** *via* fluoride-induced desilylation of silyl derivatives of *o*-hydroxybenzyl iodides **12** under mild experimental conditions (Scheme 4).

Dolatowska and Wojciechowski<sup>15</sup> reported the thermal extrusion of sulfur dioxide from 1,3-dihydrobenzo[c]thiophene-2,2-dioxides **16a** and 1,3-dihydro-2,1-benzisothiazole-2,2-dioxides **16b** to generate the corresponding quinodimethanes **17a** and quinonemethyleneimines **17b**, which undergo Diels–Alder reaction with alkene **18** to give the compound **19** (Scheme 5).

The sultone of 2-hydroxytoluene- $\alpha$ -sulfonic acid **20** after extrusion of  $\text{SO}_2$  upon photochemical irradiation gave *o*-quinone methide **21**, which upon reaction with *N*-phenyl maleimides **22** afforded the respective adducts **23** (Scheme 6).

Ohwada and co-workers<sup>16</sup> reported a retro-Diels–Alder reaction of 4*H*-1,2-benzoxazines **24** to generate *o*-QMs **25** under the thermal conditions, which undergoes the Diels–Alder reaction with vinyloxy cyclohexane **26** to afford the chroman derivative **27** (Scheme 7). They also presented a mechanistic study of the retro Diels–Alder reaction of benzoxazines **24** with various substituted benzene rings. In general, *o*-QMs are too unstable to be isolated and observed spectroscopically, unless they are trapped with metal complexes such as  $\text{Cp}^*\text{Ir}$ . In all the previously reported methods, *o*-QMs were generated *in situ*, and underwent 1,4-conjugate addition with nucleophiles or cyclo-addition reaction with suitable dienophiles.

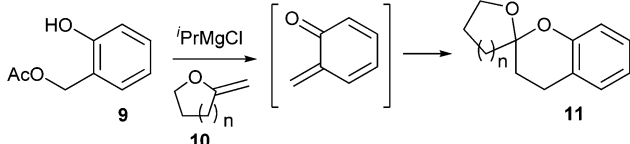
*o*-QMs may be generated through a diverse range of initiation methodologies (Scheme 8). Perhaps the most commonly encountered method for the generation of *o*-QM is the elimination of a stable molecule, typically a benzylic substituent, to generate the methylene and  $\alpha$ -carbonyl functionalities with concomitant dearomatisation. Various precursors have been utilized for the thermolytic generation of *ortho*-quinone methides. It should be noted that all thermal generation techniques preclude the application of nucleophiles that are thermally unstable. With any given precursor, there is a substantial temperature range for initiation that depends upon the substituents. In general, if the process involves significant non-bonded interactions, then the temperature requirements are higher, while extended conjugation or other stabilizing factors lower the overall temperature requirements (Scheme 8).

## 2.2. Photochemical generation

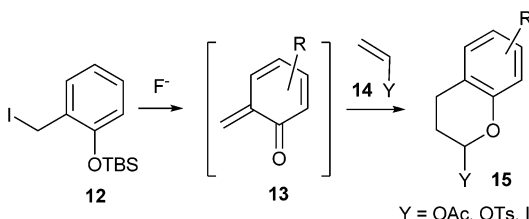
Apart from the thermal generation of *o*-QM intermediates in the presence of different basic or acidic reagents, photochemical energy sources have also been extensively used to generate *o*-QMs. In general, *o*-QM intermediate **29** is generated by light-induced water elimination from *ortho*-hydroxybenzyl alcohols **28** or by excited state intramolecular proton transfer (ESIPT) in *ortho*-hydroxystyrenes **30** (Scheme 9).

The majority of  $\beta$ -cyclodextrin inclusion complexes undergo photohydration of the olefin, preventing the formation of *o*-QM by insertion of a methylene group between the phenol and the olefin moieties. Miranda *et al.*<sup>17</sup> reported the formation of an *o*-QM *via* C–C fragmentation of a zwitterion formed by excited state intramolecular proton transfer (ESIPT) from an *ortho*-allylphenol derivative **31**, for the first time (Scheme 10). The mechanism has been explained in terms of the formation of the zwitterionic intermediate **32A** by the initial ESIPT from the phenolic subunit to the double bond. Thus, subsequent C–C bond formation with concomitant ring opening elucidates the generation of the *o*-QM **32B**, which would be trapped by solvent methanol to give compound **33**. The direct involvement of an *o*-QM intermediate has been confirmed by laser flash photolysis. Use of 266 nm excitation wavelengths in acetonitrile solvent gave a well defined signal with two maxima around 300 and 400 nm.

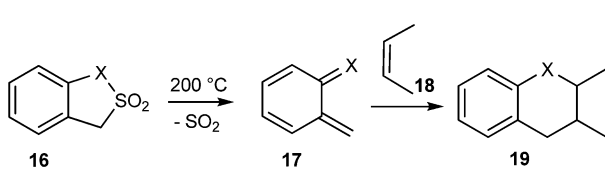
Generation of *o*-QM by flash photolysis of *ortho*-hydroxybenzyl substrates **34** in aqueous solution has also been reported (Scheme 11). Hydrogen-ion catalyzed hydration of *o*-QM



Scheme 3 Generation of *o*-QM using *o*-hydroxybenzyl acetate and *i*PrMgCl.

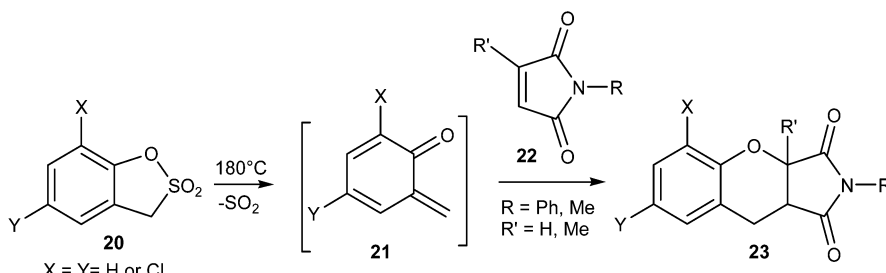
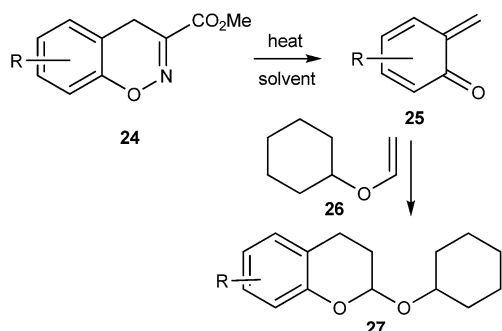
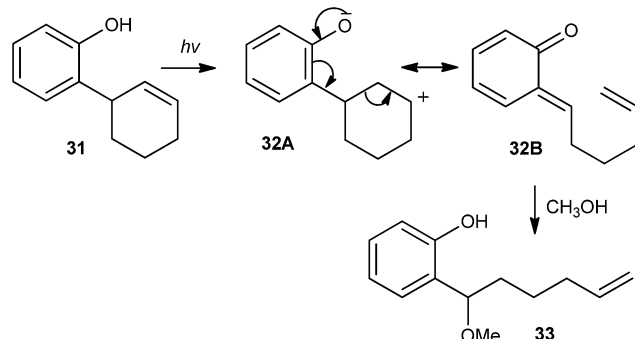
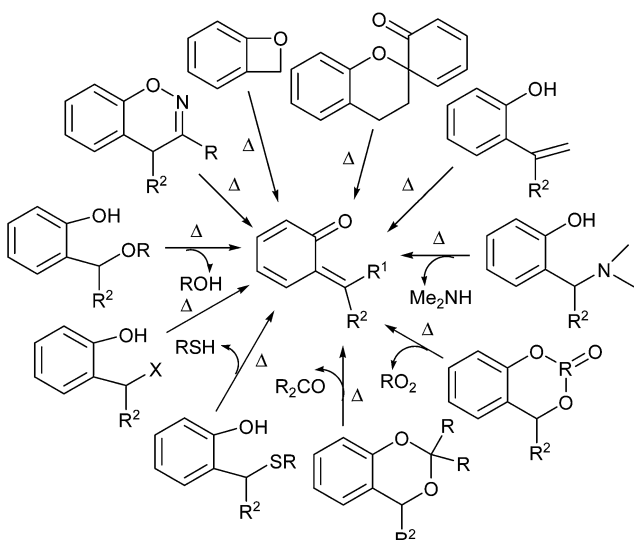
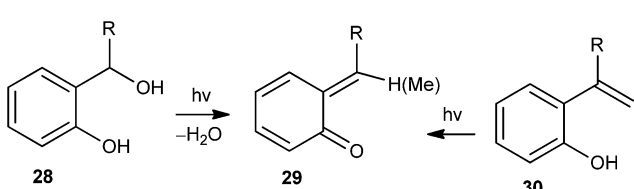
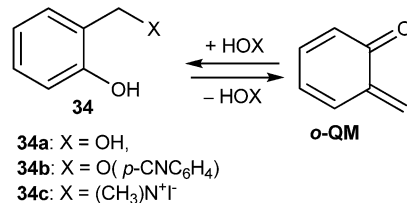


Scheme 4 Formation of *o*-QMs *via* fluoride-induced desilylation.



16a, 17a, 19a, X = CH<sub>2</sub>; 16b, 17b, 19b, X = NR

Scheme 5 Generation of *o*-QMs **17** by thermal extrusion of sulfur dioxide.

Scheme 6 Generation of *o*-QM from benzosultones.Scheme 7 Formation of *o*-QM via retro-Diels-Alder reaction of 4H-1,2-benzoxazines 24.Scheme 10 Generation of *o*-QM via C-C fragmentation of zwitterions.Scheme 8 Thermal generation of *o*-QMs.Scheme 9 Photochemical generation of *o*-QMs.Scheme 11 Flash photolysis of *o*-hydroxybenzyl substrate 34 to give *o*-QM.

Lukeman and Wan<sup>20</sup> observed predominance D<sub>2</sub>O exchange at the 2'-position irrespective of D<sub>2</sub>O (MeOD) content during the study of the photochemical incorporation of deuterium on phenylphenol **40** in D<sub>2</sub>O (CH<sub>3</sub>OD)-CH<sub>3</sub>CN solutions with varying D<sub>2</sub>O (CH<sub>3</sub>OD) content. Exchange at the 2'-position (but not at the 4'-position) was observed when crystalline samples of compound **40** (deuterated OH *i.e.* OD) were irradiated (Scheme 12).

No deuterium exchange was observed in case of compounds **49–52**, whereas 2,2'-biphenol **48** underwent similar photoexchange reaction as compound **40** (Fig. 5).

Wan and co-workers<sup>21</sup> reported the generation of quinone methide **54** by ESIPT, in which naphthyl group acts as the proton acceptor (Scheme 13). The reaction has been carried out in a variety of solvents, as well as in the solid state, illustrating that the proton transfer is intrinsic (proton transfer does not require water).

Zhan and co-workers<sup>22</sup> have reported the generation of *o*-thioquinone methide **59** by flash photolysis of benzothiote **58** in aqueous medium (Scheme 14). The hydration rates of the quinone methide **59** to *ortho*-mercaptopbenzyl alcohol **60** were measured in perchloric acid solution using H<sub>2</sub>O and D<sub>2</sub>O as the solvent in acetic acid in the presence of tris(hydroxymethyl) methylammonium ion buffers.

The solvent isotope effects on hydronium-ion catalysis of hydration for the two substrates are different. Solvent isotopic

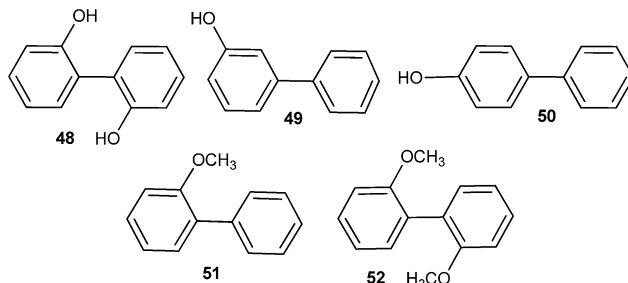
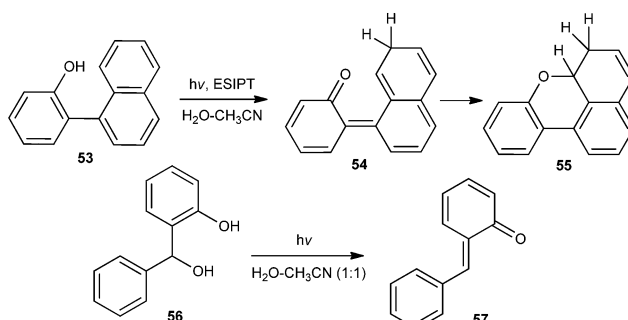


Fig. 5 Structure of compounds which do not undergo deuterium exchange.



Scheme 13 Generation of *o*-QM by ESIPT.

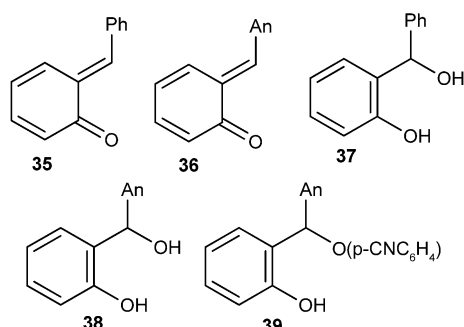
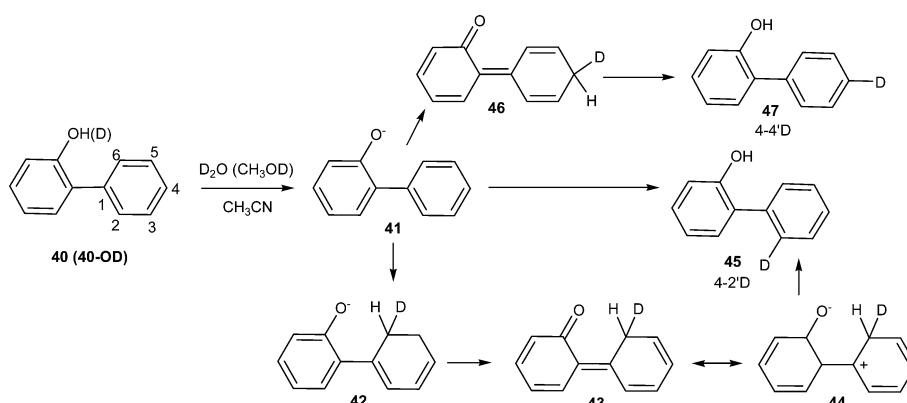


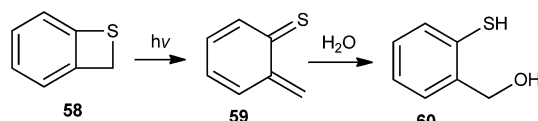
Fig. 4 Structures of *o*-hydroxybenzyl alcohols and their photo-dehydrated *o*-QMs.

effect for the oxygen quinone methide **61** is  $k_H/k_D = 0.42$ , whereas for the sulfur substrate **59** is  $k_H/k_D = 1.66$ . The inverse isotope effect ( $k_H/k_D < 1$ ) in the oxygen containing system specifies pre-equilibrium proton-transfer reaction mechanism by which protonation of the substrate on its oxygen atom being fast and reversible, and capture of the benzyl-type carbocationic intermediate is observed. On the other hand, the normal isotope effect ( $k_H/k_D > 1$ ) in the sulfur system indicates that the protonation of the substrate on its sulfur atom is rate-determining and carbocation capture is fast (Scheme 15).

Matsumoto and co-workers<sup>23</sup> reported that the thermal and photochemical generation of *o*-QM was accelerated by the presence of water molecules in the reaction solvents *via* the

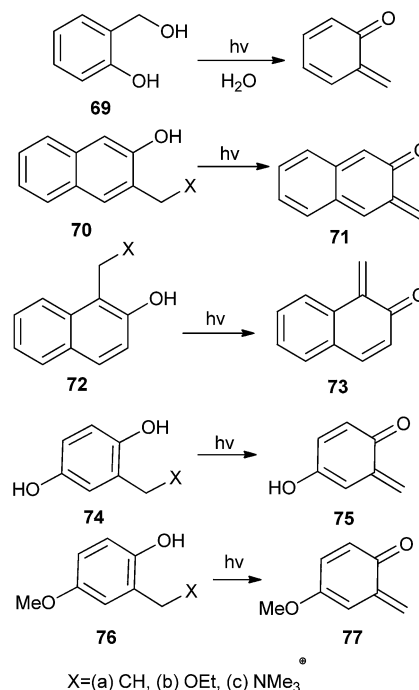
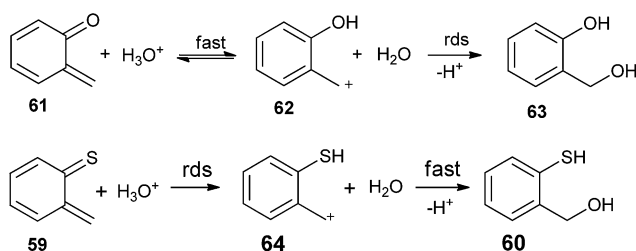


Scheme 12 Photochemical incorporation of deuterium on phenylphenol.

Scheme 14 Generation of *o*-thioquinone methide 59.

formation of anionic micelles and vesicles. According to their report, amino phenanthrol 65 and their naphthalene analogues act as precursors and transforms to QM 68 in the presence of light (Scheme 16).

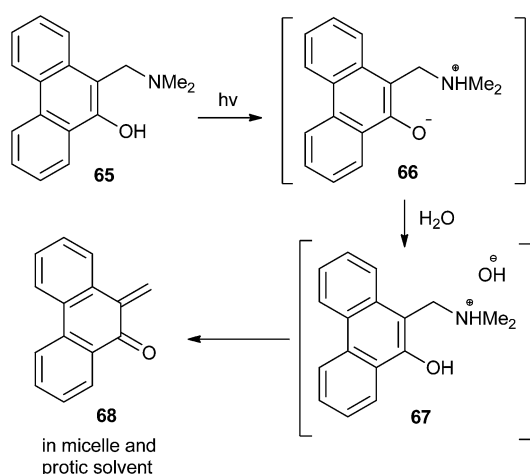
Popik and Arumugam<sup>24</sup> reported the efficient generation of quinone methide from 2-hydroxymethyl phenol 69. Isomeric 3-hydroxy-2-naphthalenemethanol 70 and 2-hydroxy-1-naphthalenemethanol 72 resulted the respective naphthaquinone methides, 2,3-naphthoquinone-3-methide 71 and 1,2-naphthoquinone-1-methide 73 (Scheme 17). During the generation of *ortho*-naphthaquinone methides (*o*-NQMs) 71 and 73 in the flash photolysis of ammonium precursors 70c and 72c ensues within the duration of a laser pulse, irradiation of 70a and 72a as well as their ethoxy derivatives 70b and 71b provides evidence for the detection of a kinetic precursor to *o*-NQMs. The rate of formation of *o*-NQMs does not depend on the pH of the solution. Furthermore, the generation of cyclohexadienone 75

Scheme 17 Generation of *o*-QM by using phenolic derivatives.Scheme 15 Solvent isotope effects on *o*-QM and *o*-thioquinone methide.

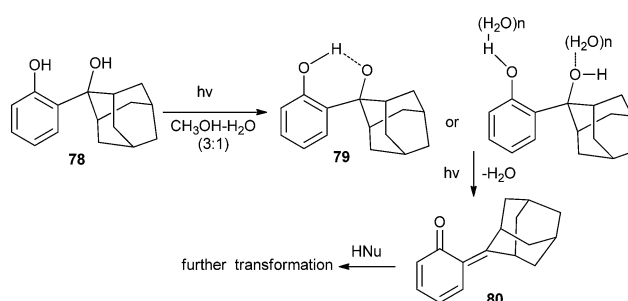
and 76 by the photochemical irradiation of three different precursors 74a-c and 76a-c have been reported (Scheme 17).

Wan and co-workers<sup>25</sup> tactically substituted the hydroxymethyl phenols with 2-hydroxy-2-adamantyl moiety and explored their photochemical reactivity. Upon the excitation of AdPh derivative 78 to its singlet excited state, it undergoes a intramolecular proton transfer at first, followed by the loss of H<sub>2</sub>O to give quinone methide 80, which has been detected by laser flash photolysis (CH<sub>3</sub>CN-H<sub>2</sub>O 1 : 1,  $\tau = 0.55$  s) and UV-vis spectroscopy (Scheme 18). The quantum yield of QM formation has been increased by three fold, and the lifetime is enhanced by the introduction of the adamantyl substituent on the *ortho*-hydroxymethyl phenol moiety.

Freccero and co-workers<sup>26</sup> reported the photogeneration of new Binol quinone methides 83 and 84. They also explored mono- and bisalkylation of free nucleophiles by product distribution analysis and laser flash photolysis in water solution using Binol quaternary ammonium derivatives 81 and 82 as photoactivated precursors (Scheme 19).

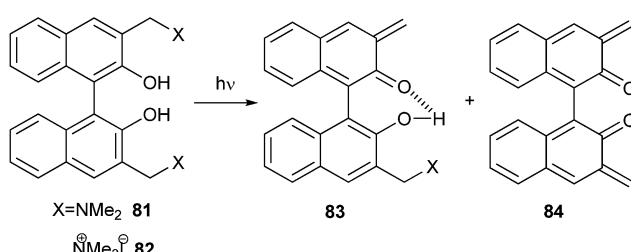


Scheme 16 Generation of QMs by the formation of anionic micelle and vesicle.

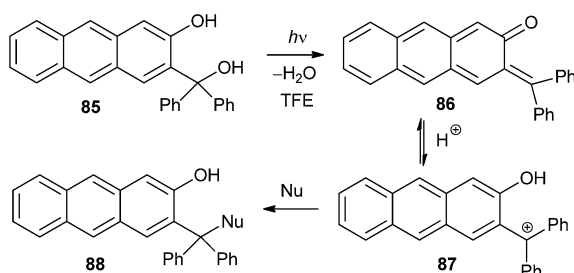
Scheme 18 Formation of adamantyl substituted *o*-QM 80.

Excitation of anthracene derivative **85** to  $S_1$  initiates photo-dehydration giving the corresponding quinone methide **86** that was detected by laser flash photolysis (LFP) in 2,2,2-trifluoroethanol.<sup>27</sup> The QM decays by protonation giving a cation **87**, which subsequently reacts with nucleophiles to give compound **88** (Scheme 20). QMs of the anthrol series is important for its potential use in biological systems because the chromophore absorbs at wavelengths  $> 400$  nm. Anti-proliferative investigations conducted with 2-anthrol derivative **85** on three human cancer cell lines showed higher activity for irradiated cells.

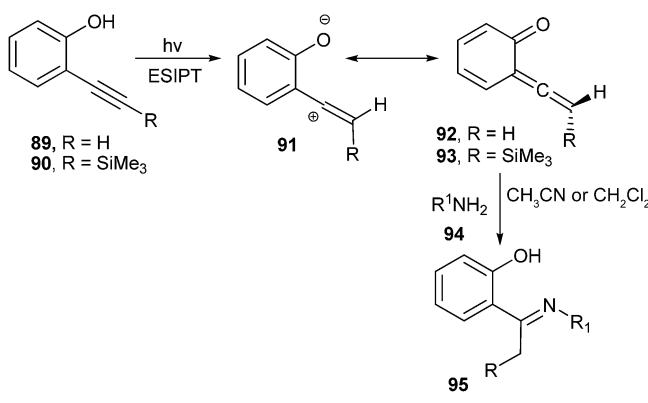
The vinylidene-quinone methides **92** and **93** were generated by irradiation of 2-alkynylphenols **89** and **90**, respectively, which were detected by laser flash photolysis in organic solvents and aqueous acetonitrile (Scheme 21).<sup>28</sup> It was also shown that the UV-vis properties and the electrophilicity are enhanced by a  $\beta$ -silicon effect and solvent polarity.



Scheme 19 Photochemical generation of binol quinone methide.



Scheme 20 Formation of QM by photodehydration of hydroxylated anthracene.



Scheme 21 Photochemical generation of vinylidene-QMs.

### 3. Reactions of *ortho*-quinone methides

The transient nature of *ortho*-quinone methides is due to their propensity to undergo rapid rearomatization, either by the Michael addition of nucleophiles or often more usefully by the cycloaddition with  $2\pi$  partners or *via* oxa-6 $\pi$ -electrocyclisation. Surprisingly, this rapid reactivity was historically seen as a deterrent to synthetic development in the field, with the potential for dimerisation and trimerisation sometimes being major stumbling block. To avert this, it is common to employ an excess of the nucleophilic or dieneophilic components and the localized *o*-QM concentration is often kept low.

*o*-QMs, being labile intermediates, have been stabilized by metal coordination. The examples of simple isolated quinone methides are rare. In fact, in condensed phases, the parent compound has only been characterized spectroscopically at lower temperatures because it is extremely reactive. Spectroscopic evidence of the zwitterionic form of the *o*-QM derived from vitamin E has only been possible at  $-78$  °C, through the stabilization by interaction with *N*-methylmorpholine *N*-oxide. These results show how difficult it is to isolate quinone methides. *para*-Quinone methides have been discussed as intermediates in the chemistry of lignins and have been used in organic synthesis as electrophiles or electron acceptors. Because the parent *o*-QM molecule is unstable, NMR spectroscopic data are not available. Therefore, the metalated parent *ortho*-quinone methide complex was examined using two-dimensional NMR spectroscopic techniques to understand its structure and reactivity. *o*-QMs are also believed to be key intermediates in the action of several antitumor and antibiotic drugs.

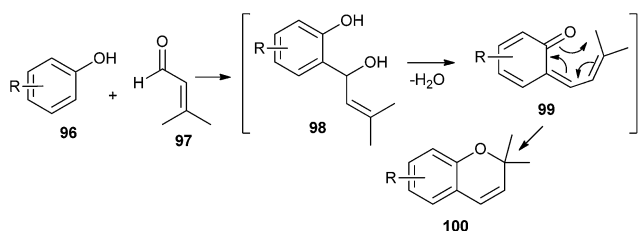
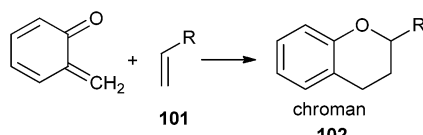
#### 3.1. Electrocyclisation and cycloadditions

**3.1.1. [4 + 2] electrocyclisation and cycloadditions.** Baldwin and Adler<sup>29</sup> have reported a proficient process for the synthesis of 2,2-dimethyl-2*H*-chromenes in a single step from the corresponding phenol and 3-methyl-2-butenal *via* microwave irradiation in  $\text{CDCl}_3$ . These reactions generated a transient *o*-QM intermediate **99**, which upon *in situ* electrocyclization gave the final bicyclic chromenes **100** in good yields (Scheme 22).

*ortho*-Quinone methides are versatile intermediates involving a minimum of seven carbon atoms, which are mainly involved in 1,4-Michael type additions as well as aza-Michael reactions with various nucleophiles. *o*-QMs also give Diels-Alder and hetero-Diels-Alder cycloaddition products (Scheme 23). *o*-QM especially derived from 4-hydroxycoumarin undergo [4 + 2] cycloaddition reaction with penta-fulvenes to afford pyranocoumarin and pyranopyrone.<sup>30</sup>

Ploypradith *et al.*<sup>31</sup> reported the generation of *o*-QMs by the reaction of compound **103** with *p*-TsOH on silica. Hetero Diels-Alder (HDA) reaction of *in situ* generated *o*-QMs **104** with styrenes **105** and **106** gave the corresponding arylchromans **107** and **108** in good yields (Scheme 24).

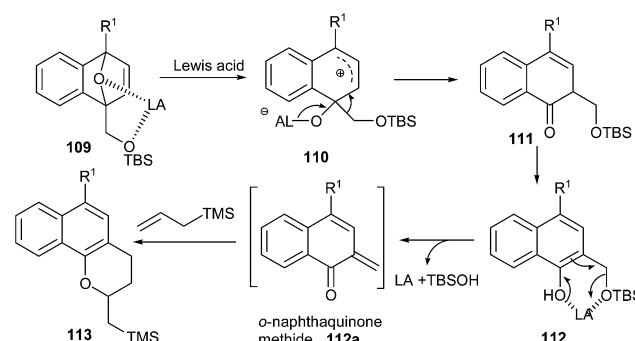
Sajiki and co-workers<sup>32</sup> established a  $\text{FeCl}_3$ -catalyzed method for the synthesis of 1-naphthoquinone-2-methides **112a** from dihydronaphthalenes **109** and further transformation of the

Scheme 22 Synthesis of chromenes via electrocyclization of *o*-QMs.Scheme 23 Reactivity of *ortho*-quinone methide with alkenes.

products in an annulation reaction with various allyl silanes to afford biologically useful dihydronaphthopyran derivatives. The annulation can proceed *via* an *o*-NQM intermediate. The site-selective cleavage of one C=O bond is promoted by the coordination of the two oxygen atoms of **109** to the Lewis acid to give a five-member ring, which is then cleaved to give the zwitterionic intermediate **110**. Subsequent migration of the siloxymethyl group (−CH<sub>2</sub>OTBS) and aromatization provides the 2-siloxymethyl-1-naphthol **112**. Further, Lewis acid induced elimination of the silanol (TBSOH) leads to an *o*-NQM **112a**, which undergoes annulation with allyl-TMS through a hetero-Diels–Alder reaction to furnish **113** (Scheme 25).

Lindsley *et al.*<sup>33</sup> reported the total synthesis of polemannones B **114** and C **115**, which are highly oxygenated benzoxanthenones derived from *Polemannia montana*, by employing a catalytic Cu(II)/sparteine oxidant system for  $\beta,\beta$ -phenolic couplings and cascade Diels–Alder reaction by tandem inverse-electron demand, producing 75–90% yield (Fig. 6).

The polemannones are unique because there is an extra electron donating ether moiety. Compounds containing

Scheme 25 FeCl<sub>3</sub>-catalyzed synthesis of 1-naphthoquinone-2-methides.

electron-donating ether moieties *para* to the phenol, such as **116**, stabilize the *o*-QM intermediate and provide the ‘push’ in the inverse-electron demand in the Diels–Alder reaction during the synthesis of **118** *via* *o*-QM **117** (Scheme 26). If two electron-donating ether moieties are present, the second one is always located at *meta* to the phenol.

But exceptionally, it is interesting that the *o*-methoxy group, as in **119**, equally stabilizes the *o*-QM intermediate and provides the ‘push’ in the inverse electron demand in the Diels–Alder reaction to provide the unnatural benzoxanthenone **121** (Scheme 27).

Jha and co-workers<sup>34</sup> reported the synthesis of naphthopyrans **133** from 2-naphthol **129**, a secondary amine **124**, and 3-hydroxy-2,2-dialkylpropanal **122** in the presence of a catalytic amount of *p*-toluenesulfonic acid. This reaction is a one-pot

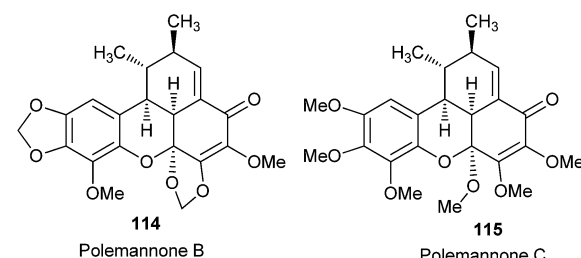
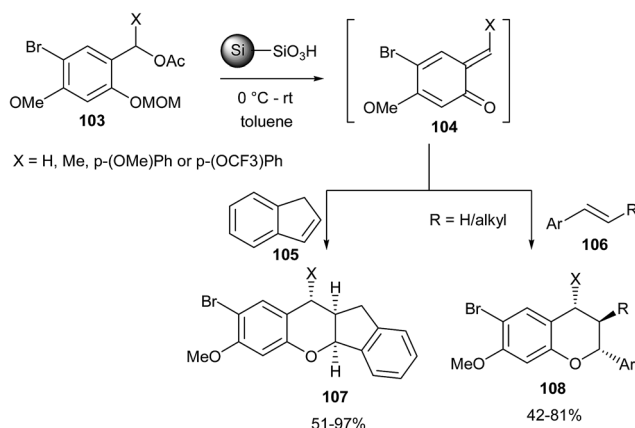
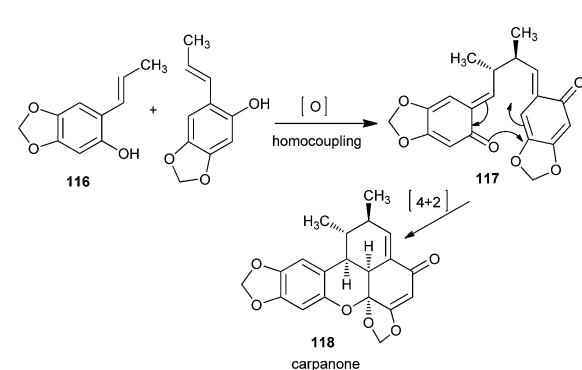


Fig. 6 Structure of polemannones.

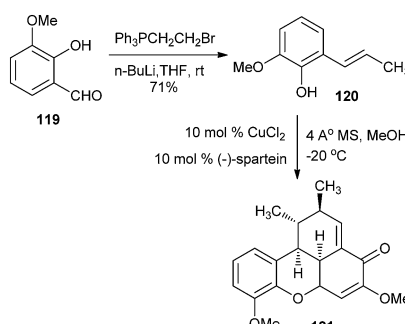
Scheme 24 Acid-catalysed generation of *o*-QMs and their HDA reaction with styrenes.Scheme 26 Synthesis of carpanone *via* electrocyclization of *o*-QM **117**.

retro-aldol disintegration of 3-hydroxy-2,2-dialkylpropanal followed by formation of a Mannich base intermediate **130** from 2-naphthol, a secondary amine, and formaldehyde (retro-aldol product). The Mannich base undergoes disproportionation to give a QM intermediate **132** and a secondary amine. Compound **125** reacts with amine **124** to generate enamine **128**. QM intermediate undergoes electrocyclization with enamines to generate the final product **133** (Scheme 28).

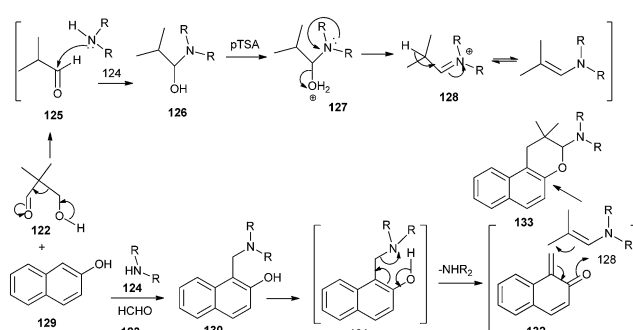
3,3-Dialkyl-2-morpholino-3,4-dihydro-2*H*-naphtho[1,2-*b*]-pyrans **137** were synthesized by the reaction of 1-naphthol **134**, morpholine **135** and compound **136** in the presence of a catalytic amount of *p*-TSA (Scheme 29).

Lee *et al.*<sup>35</sup> have reported an efficient one-pot approach for the synthesis of benzopyranobenzo pyrans and naphthopyranobenzo pyrans. Resorcinol and naphthols undergo a domino aldol type reaction followed by a hetero Diels–Alder reaction with the benzaldehyde. The reaction of compound **139** with resorcinol **140** in the presence of ethylenediamine diacetate (EDDA)/TEA first gives intermediate **141** as an aldol-type product. TEA promoted the dehydration of intermediate **141** to form quinone methides **142a** and **142b**. Because of a *sp*<sup>2</sup>-geminal effect, the endo-transition structure **142b** may be more favourable than the *exo*-transition structure **142a** due to the 1,3-allylic strain. The regiospecificity is attributed to the products **143a** and **143b** due to possibility of hydrogen bonding between the hydroxyl group and carbonyl group (Scheme 30).

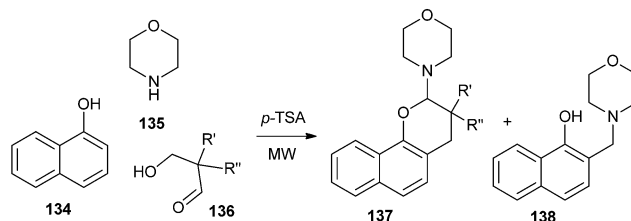
*ortho*-Quinone methide **147** arising from a formal [2 + 2] cycloaddition between aryne **144** and DMF was found to



Scheme 27 Synthesis of benzoxantheneone **121**.



Scheme 28 Synthesis of naphtha pyrans **133** via electrocyclization of *o*-QM with enamines.



Scheme 29 Synthesis of naphtho fused pyrans via *o*-QM.

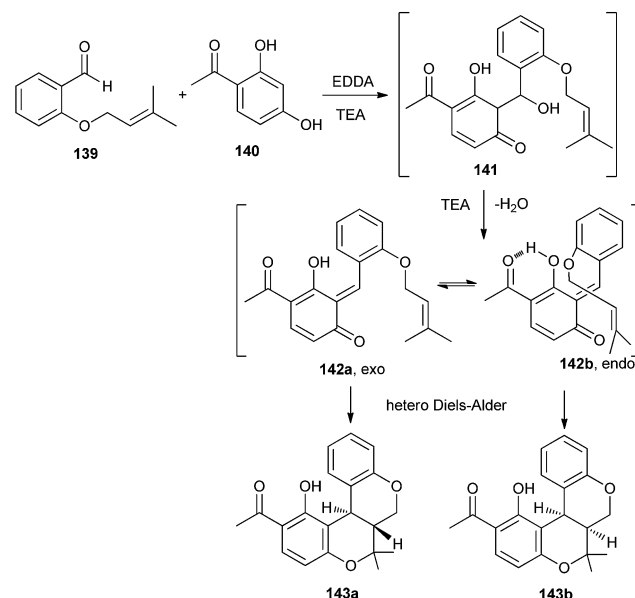
undergo a [4 + 2] cycloaddition with ester enolate **148** or ketenimine anion to produce diverse coumarins **150** (Scheme 31).<sup>36</sup>

Silver oxide-mediated oxidation of phenol substrates **151** for the synthesis of *o*-QMs **152** has been developed by Lei *et al.*<sup>37</sup> for the biomimetic syntheses of novel trimeric natural products, (±)-schefflone and tocopherol trimers **153** (Scheme 32).

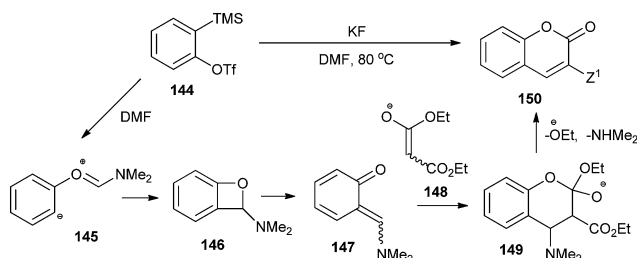
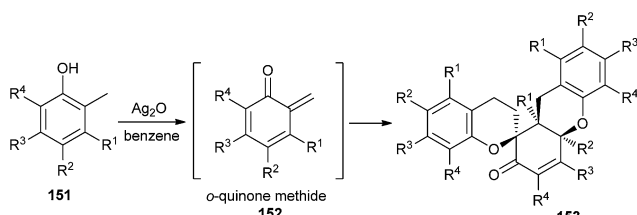
Bharate and Singh<sup>38</sup> have reported the synthesis of anti-malarial robustadials A and B **159** starting from the commercially accessible phloroglucinol. A biomimetic three-component reaction that involves the *in situ* generation of an *o*-QM via the Knoevenagel condensation followed by the Diels–Alder cycloaddition with (–)-β-pinene **157** gave robustadials A and B. A retrosynthetic pathway is shown in Scheme 33.

Robustadials A and B have been anticipated to be formed biogenetically from the Diels–Alder cycloaddition of *o*-QM **158** with (–)-β-pinene **157**. The key intermediate *o*-QM **158** could be generated by the oxidation of diformylated synthon **154** or by the coupling of phenol **155** and aldehyde **156** via a Knoevenagel condensation (Scheme 34).

The treatment of **155** with **156** and (–)-β-pinene **157** in the presence of sodium acetate in acetic acid under microwave irradiation (1000 W) for 4 min resulted in the formation of the



Scheme 30 Synthesis of benzopyranobenzo pyrans and naphthopyranobenzo pyrans.

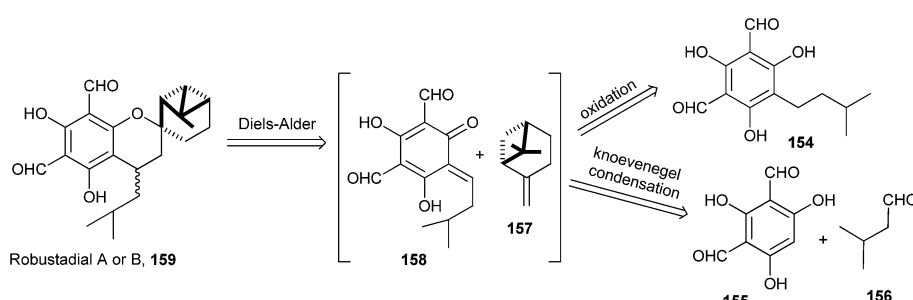
Scheme 31 [4 + 2] Cycloaddition of *o*-QM with ester enolate.Scheme 32 Silver oxide-mediated generation of *o*-QM for the synthesis of tocopherol trimers.

desired products in a combined yield of 68% (Scheme 34). Similar results were obtained when the reaction was carried out under conventional heating at 80 °C for 2 h. The *o*-QM 158 is produced *in situ* by the addition of phloroglucinol 155 with isovaleraldehyde 156 followed by dehydration (Knoevenagel-like condensation). Then 157 can undergo the cycloaddition

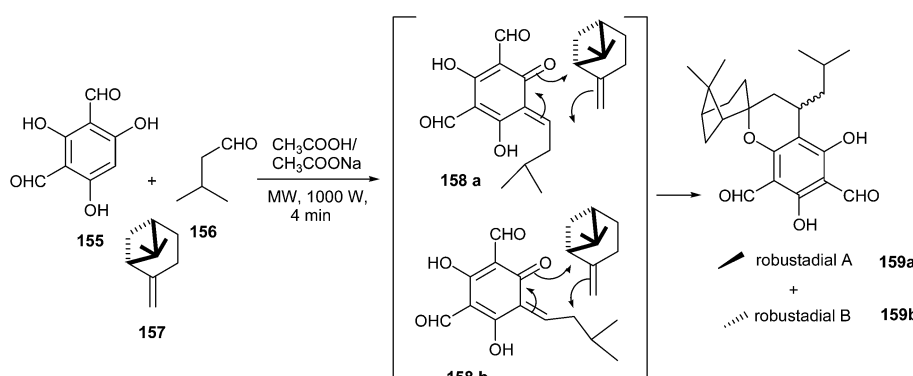
reaction with *o*-QM 158a and 158b *via* two different orientations, and each can lead to two pairs of diastereoisomers 159a and 159b. The formation of two isomers is attributed to the attack of the oxygen of the QM only to the more substituted terminus of the pinene double bond (Scheme 34).

The biosynthesis of the meroterpenoid guajadial 163 has been achieved *via* the hetero-Diels–Alder reaction between caryophyllene 160 and an *o*-QM.<sup>39</sup> Biomimetic synthesis of guajadial 163 and psidial A 164 involved a three-component coupling reaction between caryophyllene 160, benzaldehyde 161, and diformylphloroglucinol 162 in an aqueous medium (Scheme 35). It has been envisaged that the relative stereochemistry of guajadial 163 would be partly controlled by the conformation of caryophyllene 160 during the hetero-Diels–Alder reaction. The essential *o*-QM 165 could be derived retrosynthetically from a simple Knoevenagel condensation between diformylphloroglucinol 162 and benzaldehyde 161. Consequently, a domino three-component one-pot reaction between diformylphloroglucinol 162, benzaldehyde 161, and caryophyllene 160 constituted a simple biomimetic synthesis of guajadial 163.

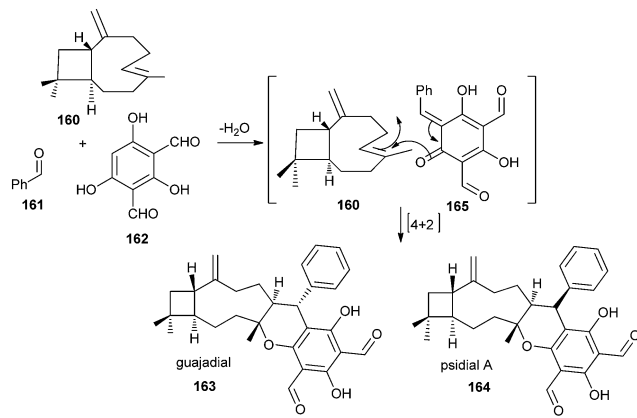
The intermolecular Diels–Alder reactions between *o*-QMs and double bonds that are not electron-rich are known to be difficult to achieve due to the easy dimerization of the *o*-QMs, which in turn accounts for the novelty and efficiency of the protocol. Caryophyllene 160 possesses a certain degree of conformational mobility; therefore, it was not certain how this flexibility would influence the facial bias in the *in vitro* hetero-Diels–Alder reaction. And from <sup>13</sup>C NMR studies and molecular mechanics calculations, we came to know that caryophyllene



Scheme 33 Retro-synthesis of Robustadials A and B.



Scheme 34 Synthesis of Robustadials A and B.

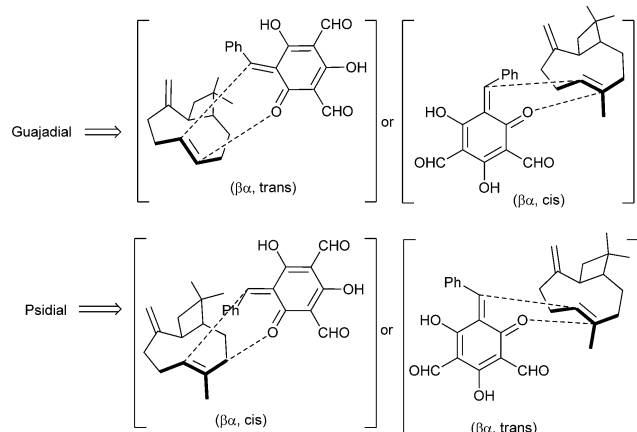


Scheme 35 Synthesis of the guajadial and psidial A.

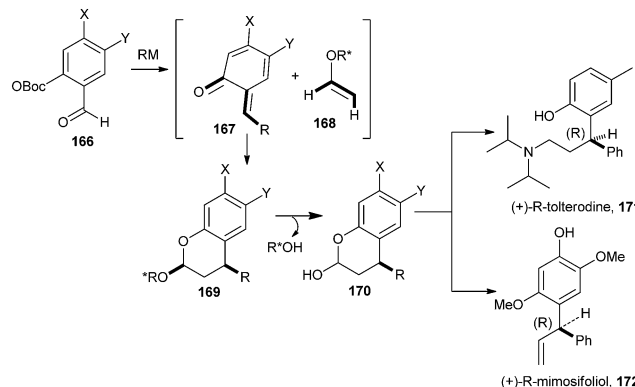
has four possible conformations ( $\alpha\alpha\alpha\beta\alpha\beta\beta$ ,  $\alpha\alpha\beta\alpha\beta\beta$ ), which vary according to the relative nature of the exocyclic methylene and olefinic methyl groups. It has been considered that the proposed biogenetic hetero-Diels–Alder reaction must involve the  $\beta\alpha$  conformer (the most stable conformer) of caryophyllene **160** with proposed transition states (Scheme 36). The stereochemical upshot of the hetero-Diels–Alder reaction was mainly controlled by the local conformation and intrinsic chirality of caryophyllene **160**.

An enantioselective cycloaddition of an *o*-QM **167** with a chiral enol ether **168** was reported for the first time by Selenski and Pettus,<sup>40</sup> and it has been portrayed along with the formal synthesis of (+)-tolterodine **171** and the total synthesis of (+)-mimosifolol **172**, as shown in Scheme 37. These syntheses demonstrate a three-component one-pot benzopyran approach for the construction of chiral benzylic junctions. A low-temperature anionic method for *o*-QM generation was achieved in high *endo/exo* ratios for ensuing cycloadditions.<sup>41</sup>

*o*-QM generation results from a series of events called the *o*-QM cascade. The cascade began with the nucleophilic addition of an organometallic reagent to an *OBoc* salicylaldehyde **166a**. The consequential benzyloxy anion **166b** attacks the *OBoc* carbonate to form a cyclic intermediate **166c**, which then



Scheme 36 Possible conformations of guajadial and psidial A.

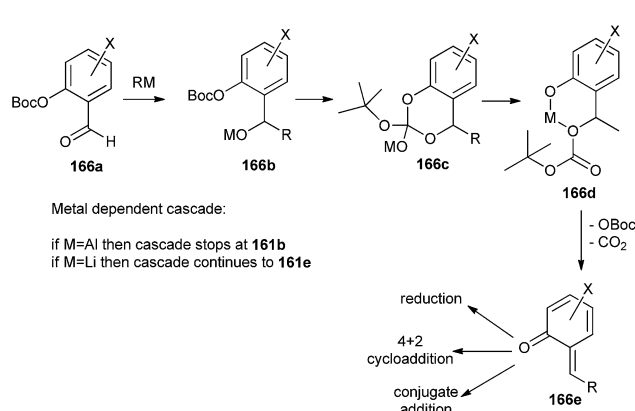


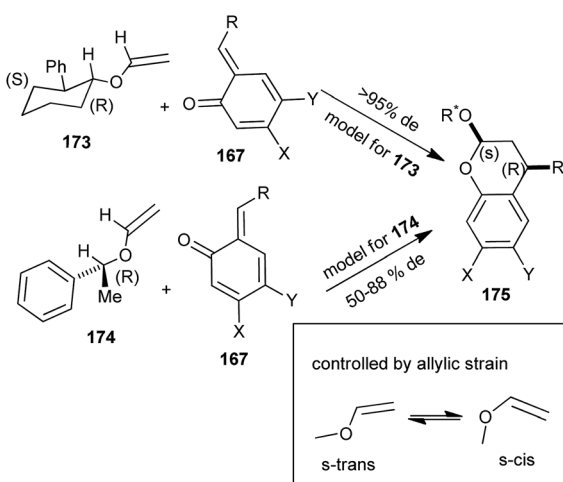
Scheme 37 Synthesis of (+)-mimosifolol.

disintegrates to form a more stable phenoxide **166d**. Within particular conditions, the  $\beta$ -elimination of the *OBoc* residue generates an *o*-QM **166e**, as shown in Scheme 38. The cascade invasion is both metal and temperature dependent and presumably represents the strength of the oxygen–metal bond and the electrophilicity of the metal cation, like an aluminium reagent proceeds to intermediate **166b**, whereas a lithium reagent leads to intermediate **166d** and a Mg reagent assists the ultimate conversion to **166e**. The consequential geometry of the *o*-QM olefin is *E*, except for a large group that is situated at the 6-position of the salicylaldehyde.

*o*-QM in the presence of chiral enol ether adduct in a dia stereoselective [4 + 2] cycloaddition. The facial selectivities of enol ethers **173** and **174** through cycloaddition are shown in Scheme 39.

The *syn* affiliation flanked by the phenyl residue of the benzopyran and the oxygen substituent of the acetal results from an *endo* transition state. By taking pseudoallylic strain and Houk's calculation into vindication, the enol ether reacts in the *s-trans* conformation. The *o*-QM endures reaction opposite the methyl residue of enol ether **173** and opposite the phenyl residue of enol ether **174**. The *S*-stereocenter of **173** and the *2R*-stereocenter of **174** induce the *S*-configuration of the resulting benzyl junction of compound **175** (Scheme 39). The absolute configuration of the chiral enol ether determines the

Scheme 38 Generation of *o*-QM using anionic method.

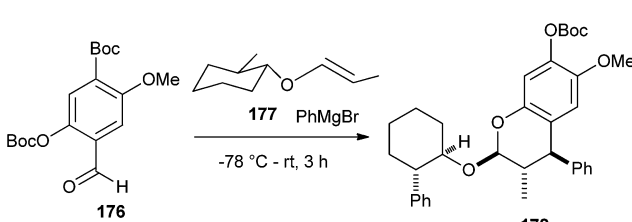
Scheme 39 Cycloaddition reaction of *o*-QM with chiral enol ether.

absolute configuration of the resulting benzopyran. The diastereoselectivity of *trans*-2S-phenyl-1*R*-cyclohexanol vinyl ether 174 was outstanding for all the *o*-QMs that ultimately created *R*-mimosifolol and *R*-tolterodine.<sup>40</sup>

The substituted enol ether 177 should also undergo a diastereoselective cycloaddition. Addition of phenyl Grignard reagent to aldehyde 176 in the presence of enol ether 177 affords benzopyran 178 creating three chiral centers with a 60% yield and 95% de (Scheme 40).

Singh and co-workers<sup>42</sup> have reported the biomimetic synthesis of *S*-Euglobals and their antileishmanial, antimalarial, and antimicrobial activities. Compound 179 was treated with formaldehyde and different terpenes like (+)-2-carene (182), (1*R*)-(-)-myrtenol (183), and (1*R*)-(-)-nopol (184) in the presence of NaOAc in CH<sub>3</sub>COOH, resulted in the development of respective pairs of regioisomers, 185 and 186 from 2-carene, 187 and 188 from myrtenol, and 189 and 190 from nopol in good yields. Similarly, treatment of 180 and 181 with formaldehyde and different terpenes in the presence of sodium acetate in acetic acid resulted in the formation of the desired cycloadducts, 191–193 and 194–196, respectively (Scheme 41).

Singh and co-workers<sup>43</sup> also described the synthesis of new analogues of euglobals 200–203 by a biomimetic approach (Scheme 42). These synthetic compounds differ from natural euglobals in the nature of monoterpene and acyl functionality. Oxidative addition of phloroglucinol-terpene with DDQ (2,3-dichloro-5,6-dicyano-1,4-benzoquinone) in nitromethane gave the corresponding *o*-QM, which further undergoes



Scheme 40 Diastereoselective synthesis of compound 178.

intermolecular cycloadditions with monoterpenes such as  $\beta$ -pinene 157,  $\alpha$ -pinene 197, (+)-3-carene 198 and (–)-camphene 199.

Kucklaendera *et al.*<sup>44</sup> reported 1,4,9,10-anthraquinone as a precursor for antitumor compounds, according to which the naphtho-condensed indoles 206 were obtained by the reactions of unsubstituted 1,4-anthraquinone 204 with enamines 205 *via* the normal Nenitzescu method. Indoles 206 were converted to Mannich bases followed by dimerization through the Diels–Alder reaction of *o*-QM intermediate 207 to give the compound 208 (Scheme 43). These synthesized heterocyclic compounds were appraised for their anticancer properties in the NCI's human disease oriented *in vitro* anticancer screen.

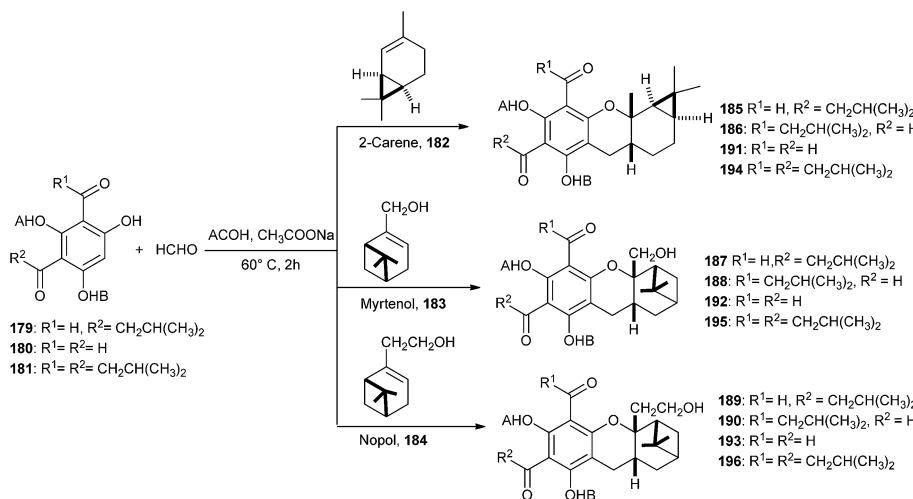
Generation of *o*-QMs by the photolysis of carboxylate derivatives 209 in aqueous acetonitrile was reported by Steinmetz and Chen.<sup>45</sup> The carboxylate leaving groups are swiftly eliminated by photolysis of the 1,4-benzoquinone 209 to produce an *o*-QM intermediate 211 that is trapped by [4 + 2] cycloaddition with unreacted starting material 209 and generated photoproduct 212. The carboxylate leaving groups are easily expelled upon photocyclisation to benzoxazolines 210 under aqueous conditions (Scheme 44).

Photolysis of 0.02 M solution of compound 209 in a mixture of 30% D<sub>2</sub>O and 70% CD<sub>3</sub>CN with a 120 W sunlamp formed benzoic acid in 58% yield with a 100% conversion rate, according to <sup>1</sup>H NMR spectroscopy. The other photoproduct 212 was formed in 36% yield, which was isolated by chromatography and identified as a 1 : 1 mixture of diastereomers by <sup>1</sup>H and <sup>13</sup>C NMR spectroscopy.

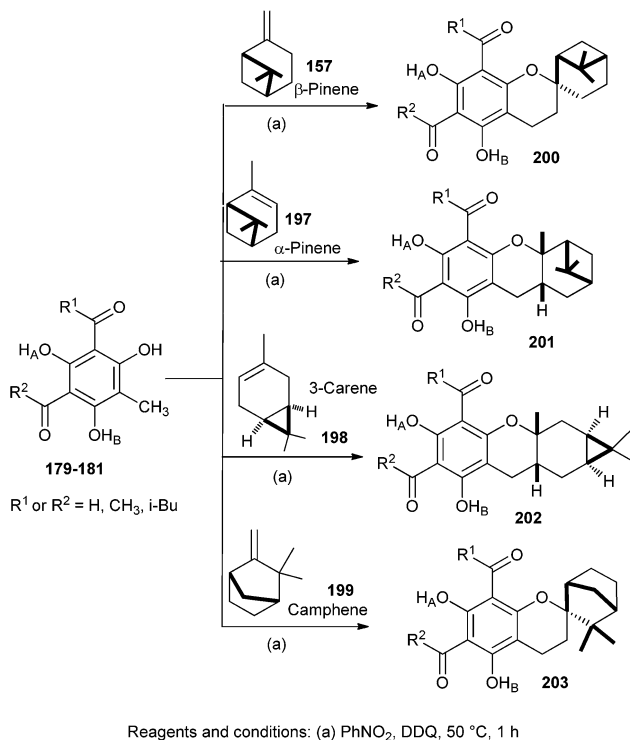
The *o*-QM intermediate 211 has been photolysed with various alkenes. Irradiation of compound 210 (10<sup>–2</sup> M) with compound 213 (0.1 M) in 30% aqueous CH<sub>3</sub>CN produced the cycloadduct 214. The cycloadduct 214 was produced in 79–87% yields at 100% conversion rates of the reactants (Scheme 45). Other alkene trapping reagents, such as dihydropyran, ethyl vinyl ether, methyl trimethylsilyl dimethylketene acetal, and diethyl fumarate, were inadequately reactive in trapping the *o*-QM, which was deactivated by multiple electron-releasing substituents.

The immediate precursor in the photocyclization to benzoxazoline 210 is zwitterionic in character in ground state as with structure 216. From photochemistry of  $\alpha$ -keto amides it has been shown that intermediates analogous to 216 can cyclize as well as expel phenolate or carboxylate leaving groups (Scheme 46). The mechanism for elimination of carboxylate leaving groups to form *o*-QM 211 is uncertain, because the elimination is possible either from 216 or 210. No evidence could be obtained to support the direct elimination of carboxylate leaving groups from 216 using nanosecond laser flash photolysis methods.

Barrero and co-workers<sup>46</sup> reported the synthesis of bioactive pupehediene derivatives involving a hetero Diels–Alder cycloaddition of *o*-QM, which was generated by the fluoride-induced desilylation of silyl derivatives of *o*-hydroxybenzyl iodides. In this protocol, two variations were investigated. At first, the compound 218 was reacted with dienophiles 219 and 221, and it was found that the reaction proceeded *via* the formation of 220 and 222. It has also been revealed that *o*-QMs undergo [4 + 2] cycloadditions with ethers 219 and 221,



Scheme 41 Biomimetic synthesis of S-euglobals.

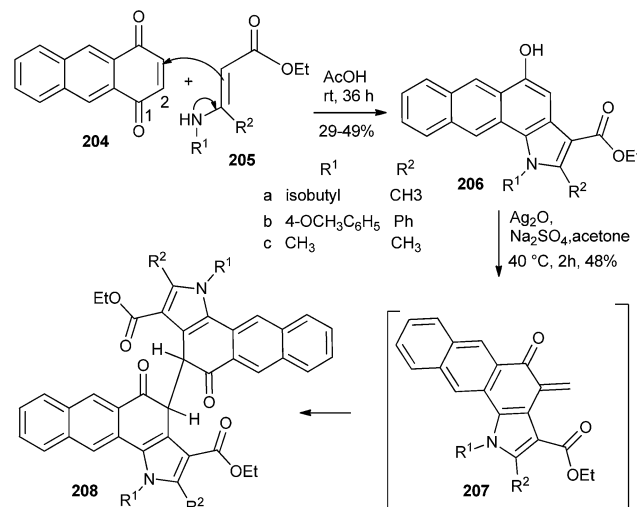


Scheme 42 Biomimetic synthesis of S-euglobals analogues.

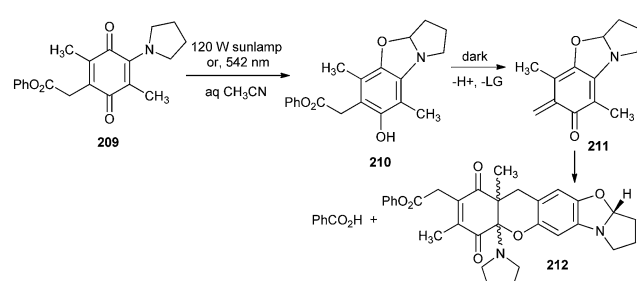
acting as dienophiles during the course of the reaction (Scheme 47).

In the second attempt, variations were introduced to explore the scope of this procedure by using different oxadienic moieties. Thus, *ortho*-silyloxybenzyl iodide, 226 was obtained from commercial 2-hydroxybenzaldehyde 224. When this compound was treated with ethyl vinyl ether, the reaction proceeded in a similar fashion to give chroman 227 exclusively (Scheme 48).

The unstable 3-methylenepyridin-4-one intermediate 233 has been developed by Baldwin and co-workers<sup>47</sup> by heating the di-Boc-pyridin-4-one derivative 232. The intermediate 233

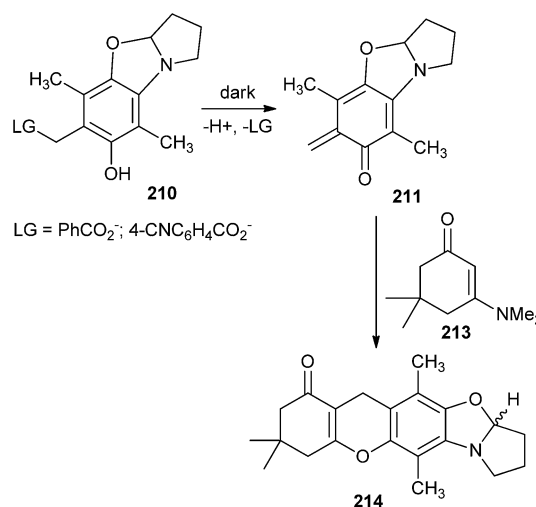


Scheme 43 Synthesis of naphtho-condensed indoles.



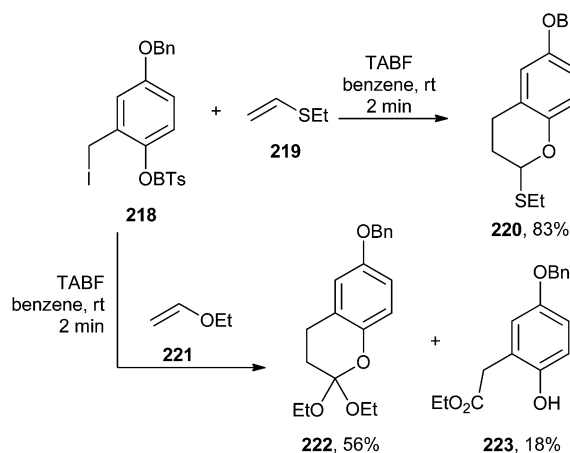
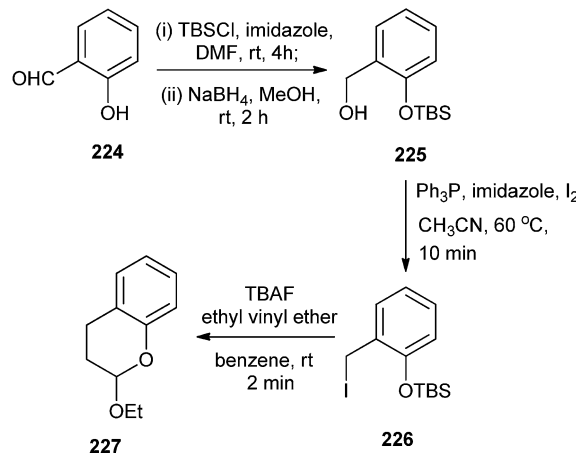
Scheme 44 Synthesis of compound 212 via photogenerated o-QM.

undergoes rearomatization followed by the Diels–Alder cycloaddition with activated alkenes to give substituted pyrano[3,2-*c*]-pyridines 234. The precursor 231 for the synthesis of 234 was obtained from commercially available 4-methoxypyridine 228. Formylation of 228 gives 229, which after reduction furnished compound 230 (Scheme 49).

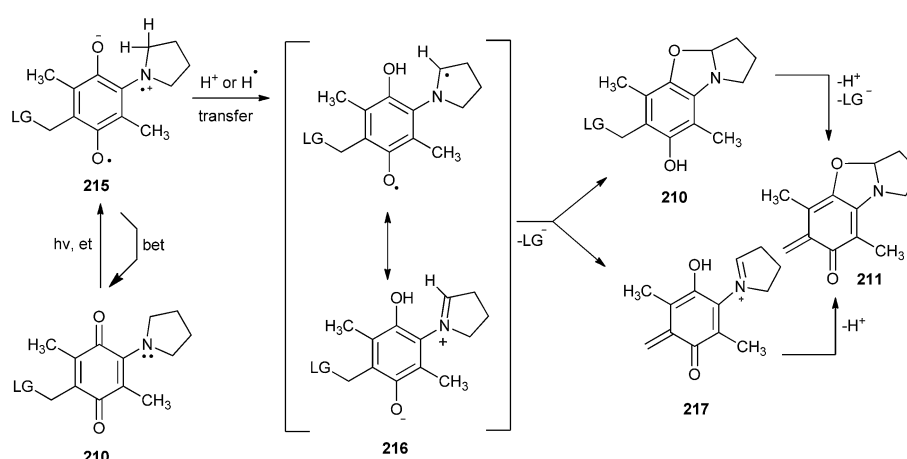
Scheme 45 Photolysis of *o*-QM 211 with alkene.

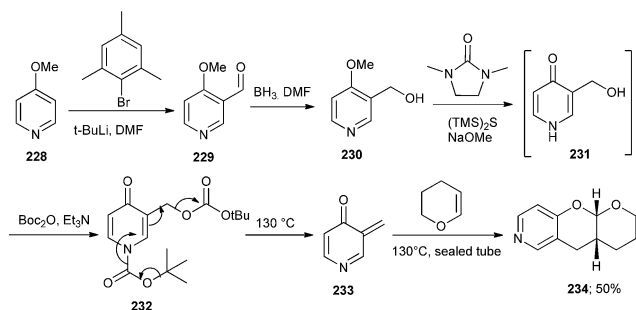
Unusual hetero Diels–Alder reactions between various electron-rich oxazoles and *o*-QMs have been achieved by Lindsey and Pettus.<sup>48</sup> In this case, the *o*-QM intermediate has been generated by deprotonation of either of the *ortho*-OBoc hydroxymethyl aromatic compounds (240 or 241, 0.1 M in  $\text{Et}_2\text{O}$  or THF) with *tert*-butyl magnesium bromide, which led to the migration of  $-\text{OBoc}$  and subsequent  $\beta$ -elimination (Scheme 50). Even though these *o*-QM species are extremely reactive, 4-methyl-oxazole 235 proved futile as a nucleophile. Instead, the *o*-QM intermediate undergoes self-destruction *via* known manifolds such as Diels–Alder dimerization and trimerization. The generation of *o*-QM 243 from compound 241 in the presence of oxazole 237 led to two adducts in a 62% combined yield. In this case, the 1,4-addition product prevails in the mixture and the [4 + 2] cycloadduct 245 arises in small amounts (1 : 10, 245 : 246), as shown in Scheme 50.

Surprisingly, silylated 4-hydroxymethyl oxazole 247 undergoes reaction with *o*-QM 242 to afford a 66% combined yield with a 3 : 1 mixture, favouring the [4 + 2] adduct 249 over the 1,4-conjugate addition product 250. In addition, the

Scheme 47 [4 + 2] Cycloadditions of *o*-QM with ethers.Scheme 48 Synthesis of chroman by the reaction of *o*-QM and ethyl vinyl ether.

carbonate protected 4-hydroxymethyl oxazole 248 undergoes cycloaddition with *o*-QM 243, affording benzopyran 251 in a 46% yield as the only identifiable product (Scheme 51).

Scheme 46 Mechanistic analysis for the generation of *o*-QM 211.



Scheme 49 Diels–Alder cycloaddition of *o*-QM with activated alkenes.

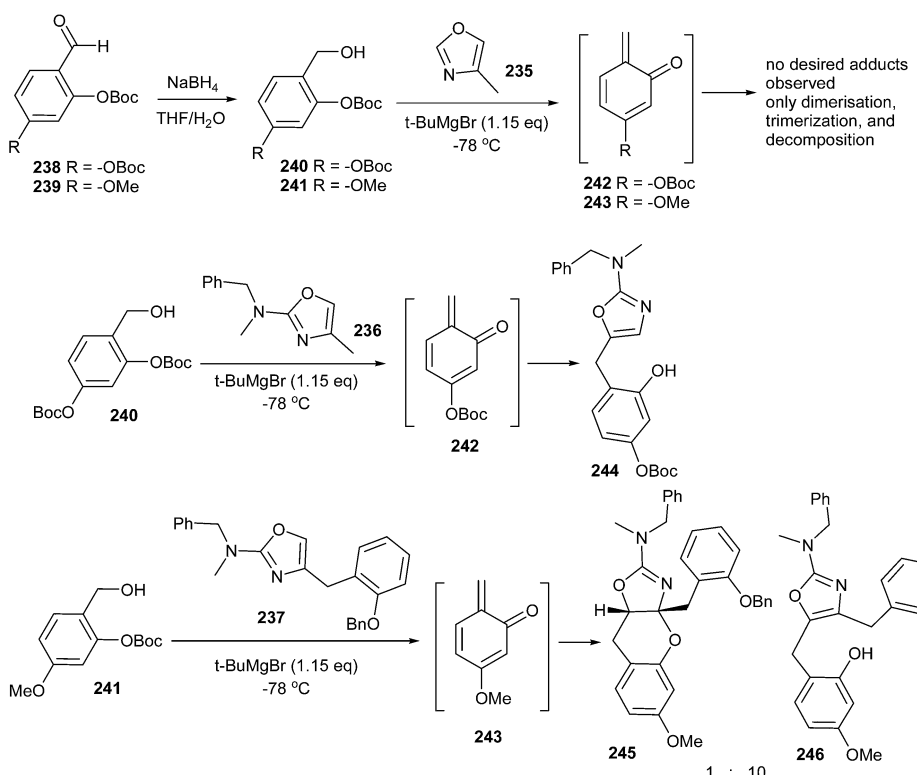
The 2-amino oxazoles displaying an electron-rich substituent at the 4-position ( $R = H, Bn$ ) underwent highly asynchronous reactions, leading to 1,4-conjugate addition adducts, whereas the oxazoles displaying an electron-withdrawing substituent at the 4-position ( $R = -OTBS, -OCO_2Et$ ) underwent a synchronous reaction, affording the [4 + 2]cycloadduct (Scheme 52).

Moreover, the *o*-QM derived from tocopherol was trapped with DNMM (4-methyl-3,4-dihydro-2*H*-[1,4]oxazine) 256 *via* the hetero-Diels–Alder reaction with inverse electron demand, and confirmed that compound 256 occurs as a degradation product of *N*-methylmorpholine-*N*-oxide.<sup>49</sup> As dehydro-NMM is an electron-rich olefin and *o*-QM is electron deficient, the hetero-Diels–Alder reaction of *o*-QM with ethyl vinyl ether proceeds regioselectively in a particular way, so that the  $\alpha$ -carbon of the vinyl reacts with the oxygen and the vinylic  $\beta$ -carbon reacts with

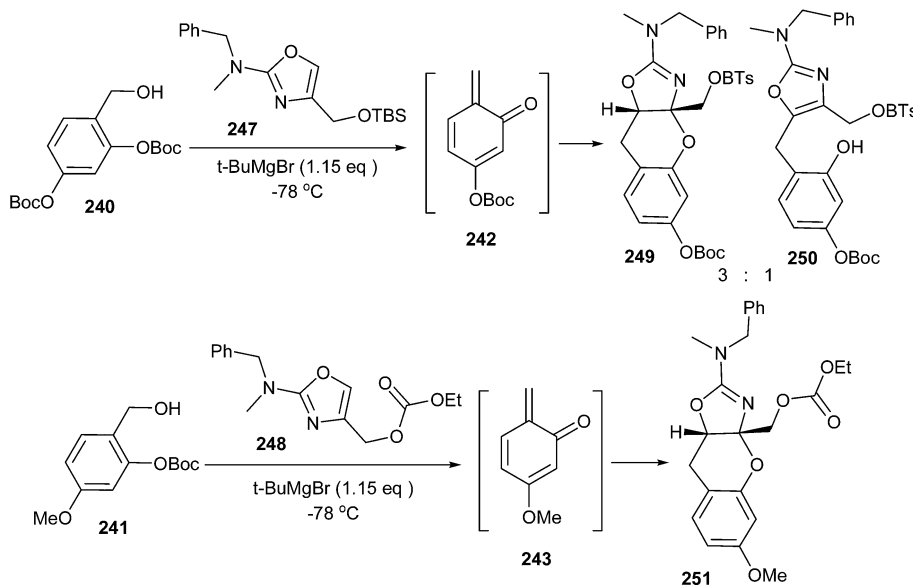
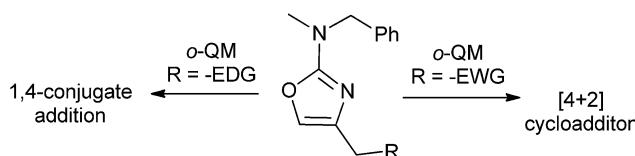
the methylene carbon of the QM.<sup>49b</sup> But in the case of DNMM 256, the situation was less unequivocal, as the compound contains both a vinyl ether and an enamine; hence, two directions of addition with *o*-QMs 254 and 255 took place, leading to tetracycles 257–260. Computations on the DFT level was performed on the shortened model compounds 255, 258, and 260, possessing a methyl group instead of the isoprenoid side chain that predicted 260 to be 12.6 kJ mol<sup>−1</sup> more stable than 258 (Scheme 53).

A mechanistically interesting enantioselective [4 + 2] cycloaddition of *o*-QM with silyl ketene acetals by catalytic pathway is well described in a previously reported method,<sup>50</sup> and was initiated by a chiral cinchona alkaloid-derived ammonium fluoride “precatalyst” complex to afford a variety of alkyl- and aryl-substituted 3,4-dihydrocoumarin products in excellent yields with good enantioselectivity. The electron-rich *o*-QM 261 was first generated by Jurd in 1977 by the reaction of sesamol and 4-methoxybenzyl alcohol under the mild Friedel–Crafts conditions followed by  $Ag_2O$  oxidation. Then, the newly generated *o*-QM 261 was treated with butyryl chloride, thermodynamic Hunig's base, which generates stable enolate and kinetic base/chiral catalyst benzoylquinidine (BQd) 262. It has been found that the high electron density on *o*-QM was not compatible with the mild nucleophilic zwitterionic ketene enolate 262; therefore, silyl ketene acetal 263 was used as the ketene enolate precursor to synthesize the compound 267 (Schemes 54 and 55).

Next, reaction of *o*-QM 261 with 263 in the presence of catalytic tetrabutylammonium fluoride (TBAF) in THF afforded



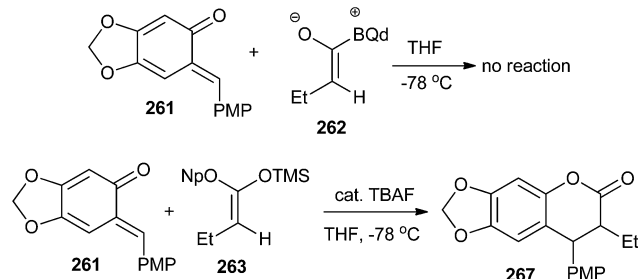
Scheme 50 Hetero-Diels–Alder reactions between various electron-rich oxazoles and *o*-QMs.

Scheme 51 Reaction of substituted oxazoles with *o*-QM.

Scheme 52 [4 + 2] Cycloadduct of oxazole derivatives.

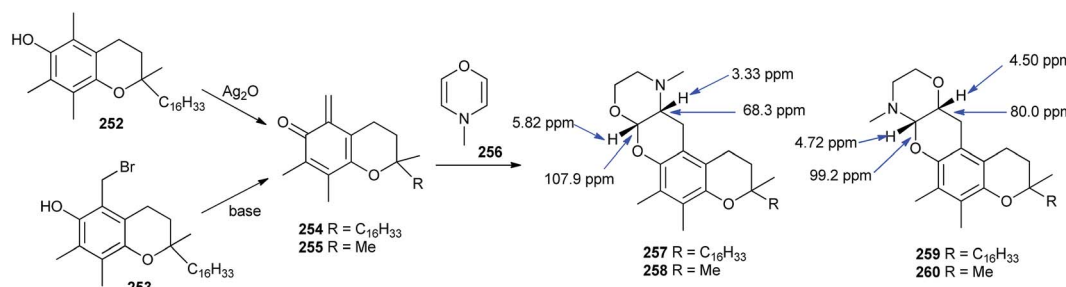
the cycloaddition product **267** with 80% ee. Thus, it shows that the precatalyst's effect on the enantioselectivity of the reaction was not dictated by steric bulk, but rather by electronic effects (Scheme 55).

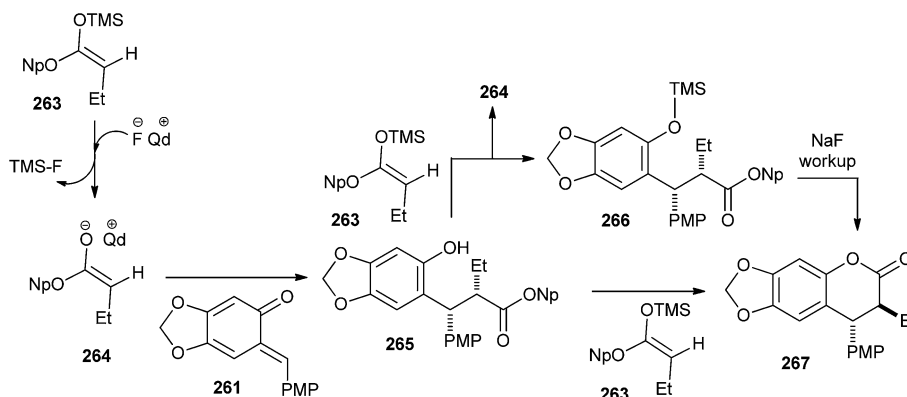
A variety of chroman spiroketals have been synthesized by Pettus and co-workers<sup>51</sup> via inverse-demand [4 + 2] cycloaddition of enol ethers with *o*-QMs. At low temperature, *in situ* generation of *o*-QM allows the kinetic diastereoselective construction of these motifs, providing entry to a number of unusual chroman spiroketals. When benzyl alcohol **269** (0.1 M in toluene, -78 °C) and 2–4 equivalents of the 1,3-dihydroisobenzofuran enol ether **268** were treated with *t*-BuMgCl, an endo-selective cycloaddition took place as the reaction mixture slowly increases to room temperature (Scheme 56). The reaction

Scheme 54 Synthesis of compound **267** utilizing silyl ketene acetal **263** and *o*-QM **261**.

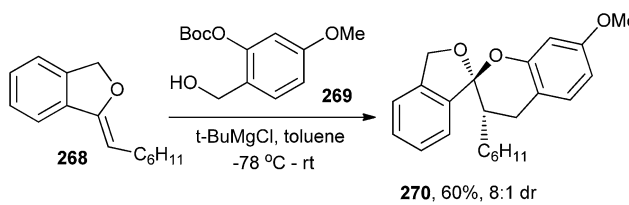
cleanly produced the chroman spiroketal **270** in 60% isolated yield (>8 : 1 dr).

The simple *exo*-enol ethers readily equilibrate with their *endo*-isomers under acidic and sometimes also thermal conditions. The major product was the expected benzopyran **273**, and the mono-benzannulated spiroketal **274** (as a mixture of diastereomers) was observed in a 25% yield during the reaction of compound **271** with *endo*-enol ether **272**. Apparently, this was the result of the cycloaddition of the intermediate *o*-QM with 4,5-dihydro-2,4-dimethylfuran (Scheme 57).<sup>12,13</sup>

Scheme 53 Reaction of *o*-QM (derived from tocopherol) with oxazine.



Scheme 55 Enantioselective synthesis of compound 267.

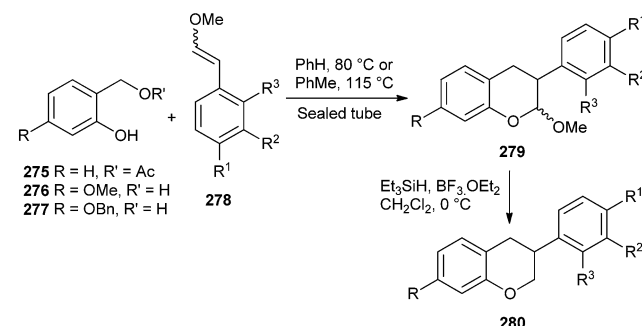


Scheme 56 Synthesis of chroman spiroketal.

The intermediacy of *o*-QM has been employed to develop a concise strategy for the synthesis of isoflavans *via* the Diels–Alder reaction between *o*-QM and aryl-substituted enol ethers 278 followed by the reductive cleavage of the acetal group.<sup>52</sup> The method is extended toward the total syntheses of equol, 3'-hydroxyequol, and vestitol. A reductive removal of the methoxy group from acetal 279 was achieved by using  $\text{BF}_3 \cdot \text{OEt}_2$  and triethylsilane to give isoflavan 280 (Scheme 58).

It has been envisioned that the Lewis acid should be able to catalyze both the [4 + 2] cycloaddition and the reductive removal of the methoxy group of the acetal moiety in a one-pot transformation. In this course, the reaction of phenol 277 and enol ether 278a with  $\text{BF}_3 \cdot \text{OEt}_2$  in  $\text{CH}_2\text{Cl}_2$  at 0 °C in the presence of triethylsilane in the same pot gave isoflavan 280a in a 34% yield (Scheme 59).

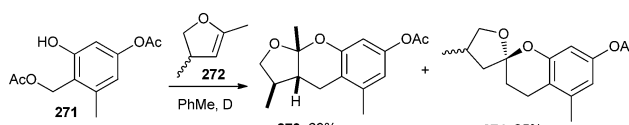
**3.1.2. [4 + 4] Cycloaddition.** A one-pot [4 + 4] cyclization pathway for the generation of eight-membered sultams *via* *in situ* generated *o*-QM was reported by Hanson and co-workers.<sup>53</sup> They examined the pairing of ambiphilic synthons in a complementary fashion, whereby *o*-fluorobenzenesulfonamides 281 were merged with *in situ* generated *o*-QM 283 (from compound 282) in a formal [4 + 4] cyclization pathway to afford dibenzoxathiazocine dioxides 284 under microwave (MW)

Scheme 58 Synthesis of isoflavan 280 *via* intermediacy of *o*-QM.

Scheme 59 [4 + 2] Cycloaddition reaction of substituted phenol with enol ether 278a.

conditions (Scheme 60). This is the first report representing the use of an *o*-QM in a formal hetero [4 + 4] cyclization.

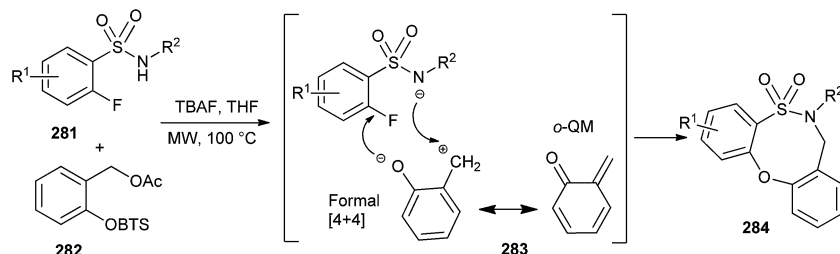
**3.1.3. [5 + 2] Cycloaddition (phenoxonium analogous to *o*-QM).** Green and Pettus<sup>54</sup> have synthesised  $\alpha$ -Cedrene,  $\alpha$ -Pipitzol, and *sec*-Cedrenol by the oxidative dearomatization-induced [5 + 2] cycloaddition. Phenols with various *ortho*-(pent-4-enyl) substitutions were directly prepared from salicylaldehydes by low temperature *o*-QM generation and consumption. The key conversion attributed to the oxidative dearomatization of an *ortho*-(pent-4-enyl)-phenol 285, followed by an intramolecular [5 + 2] cycloaddition of the respective phenoxonium intermediates 287 across the attached olefin, affords the respective derivatives of skeleton 289 (Scheme 61).



Scheme 57 Synthesis of benzopyran 273 and mono-benzannulated spiroketal 274.

### 3.2. Addition of nucleophiles

Bromination of  $\alpha$ -tocopherol 290 for the formation of 294 is not possible by simple bromination because an ethano-dimer of



Scheme 60 Synthesis of 5,2,1-dibenzoxathiazocine-2,2-dioxides by hetero [4 + 4] cyclization.

$\alpha$ -tocopherol **290** after bromination affords pyrano-spirodimer of  $\alpha$ -tocopherol **291** in > 95% yields. Compound **290** and **291** constitute a largely reversible redox pair.<sup>55</sup> Bromine oxidizes one  $\alpha$ -tocopherol **290** to an *ortho*-quinone methide (*o*-QM) intermediate **292**, which is immediately attacked by the phenolic OH group of the tocopherol. It is evidently favoured over the 1,4-addition of evolving HBr by a pre-organizational effect, as the ethano-bridge keeps the two reacting moieties in close distance. This acid facilitates the opening of **291** to regenerate the *o*-QM **292**.<sup>56</sup> Thus, the OH group was protected by TMS, which continuously traps a small percentage of the *o*-QM intermediate present and cannot react back to give compound **291**. In this way, **291** is eventually completely converted into **293** (Scheme 62). Further reaction of **293** with elemental bromine followed by desilylation provided the target bisbromide **294**.

The pseudo three-component condensation reaction of 2-naphthol with aldehydes in the presence of various catalysts to form xanthenes has been widely studied. The reaction proceeds through the *in situ* formation of *o*-QMs with 2-naphthol acting as a nucleophile. However, the three-component condensation reactions of 2-naphthol and aldehydes with other nucleophiles are rarely reported in previously studied reports. Singh and co-workers<sup>57</sup> generated substituted xanthenes **297** by one-pot condensation of 2-naphthol with aliphatic/aromatic aldehydes **295** in the presence of  $P_2O_5$  or  $InCl_3$  as catalysts under solvent-free conditions. They also reported a one-pot synthesis of tetrahydrobenzoxanthene **299** and diazabenzanthracenedione **300** in the presence of an Indium(III) chloride catalyst by a three-component cyclocondensation of aldehydes **295**,  $\beta$ -naphthol **296** and cyclic 1,3-

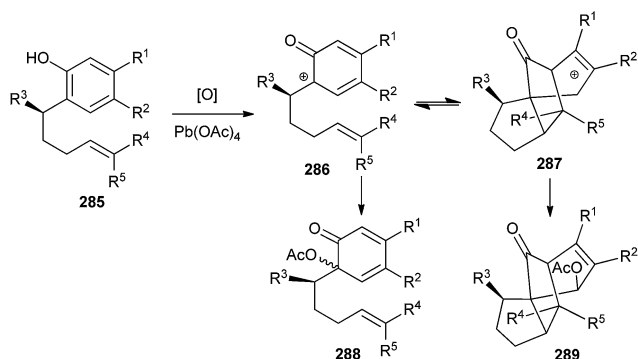
dicarbonyl compounds **298** under solvent-free conditions in high yields. This transformation has also been effectively carried out by using  $P_2O_5$  as a catalyst. The use of aldehyde **295**,  $\beta$ -naphthol **296**, and 3-oxo-3-phenyldithiopropionic acid methyl ester **301** in equimolar amounts in the presence of  $InCl_3$  produces benzo[*f*]chromene **302** in good yields (Scheme 63).

The nucleophilic addition of  $\beta$ -naphthol **296** to aldehyde **295** in the presence of  $InCl_3$  gives naphthoquinone methide intermediate **303**, which then reacts with the nucleophile like 1,3-dicarbonyl compound **298** followed by the addition of the phenolic hydroxyl moiety to the carbonyl of ketone, providing cyclic hemiketal, which on dehydration afforded **309** (Scheme 64).

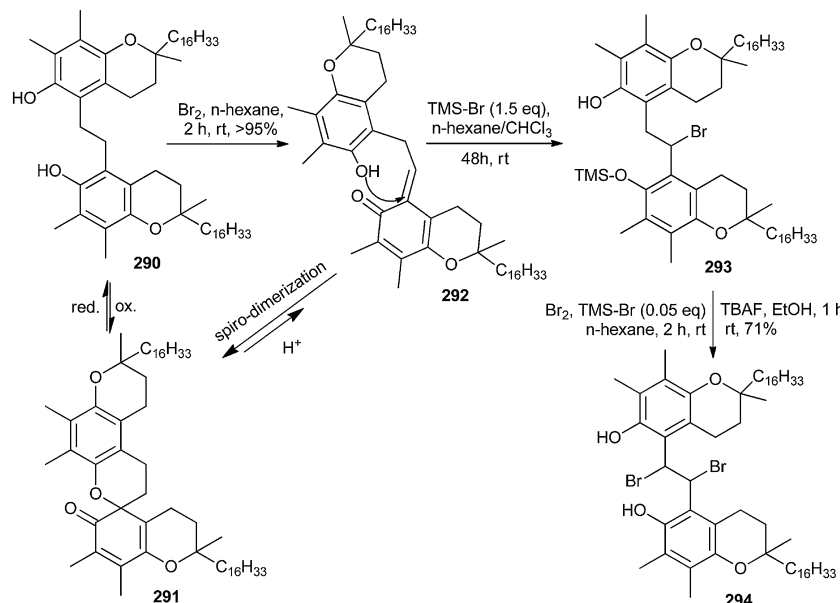
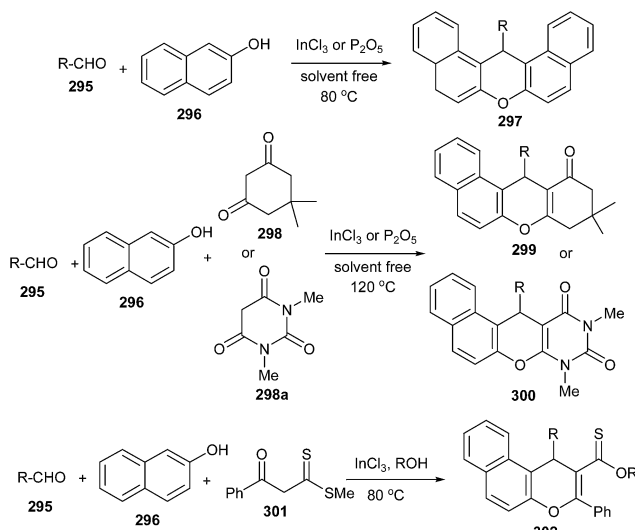
The *in situ* formation of *o*-QM intermediates in the presence of solid silica chloride under sonication followed by the nucleophilic attack of amide has been reported to lead to the formation of amidoalkyl-2-naphthol.<sup>58</sup> Due to the collapse of the cavitation bubbles near the surface of the catalyst, the oxygen of the carbonyl group might have easily replaced the chlorine atom present on the catalyst silica chloride to give the activated aldehyde, which could be attacked by  $\beta$ -naphthol to give *o*-QM **307**. Thus, the *in situ* generated *o*-QM **307** upon reaction with amide **308** furnished the envisioned amidoalkyl naphthol **309** (Scheme 65). This reaction was previously reported under the influence of  $P_2O_5$ , which acts as a catalyst as well as a water scavenger.<sup>59</sup>

Nagawade and Shinde<sup>60</sup> reported the rapid synthesis of biologically significant amidoalkyl naphthols using a catalytic amount of iodine. Chlorinated solvents (dichloroethane > dichloromethane > chloroform) gave the highest yields. The yields of the end products depend on the polarity of the solvent used, and after a thorough screening, 1,2-dichloroethane was found to be the best solvent for the protocol. *o*-QM has also been generated by the treatment of  $\beta$ -naphthol, aryl aldehyde and ureas or amides in the presence of catalytic amounts of *p*-TSA at 125 °C.<sup>61</sup> In addition to that hafnium(IV) bis(perfluorooctanesulfonyl)imide complex,<sup>62</sup> ( $Hf(NPF_2)_4$ ),  $NaHSO_4 \cdot H_2O$ <sup>63</sup> and  $H_3PW_{12}O_{40}$  have also been shown to be effective catalysts for the same reaction, with respect to reaction times and yields in the molten salt media.<sup>64</sup>

2'-Aminobenzothiazolomethyl naphthols or 5-(2'-aminobenzothiazolomethyl)-6-hydroxyquinolines **313** was prepared by the reaction of *o*-QM **312**, and 2-aminobenzothiazole. *o*-QM was generated *in situ* from the reaction of  $\beta$ -naphthol or 6-hydroxyquinoline and aldehyde **311** (Scheme 66).<sup>65</sup>

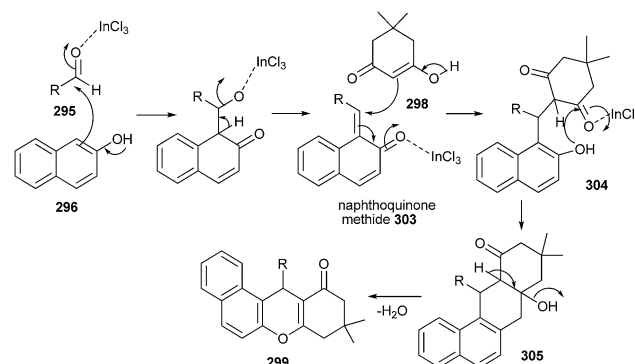
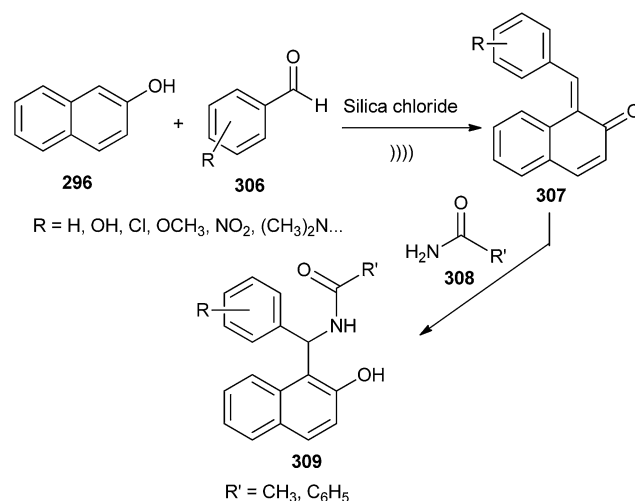


Scheme 61 Intramolecular [5 + 2] cycloaddition of phenoxonium intermediates.

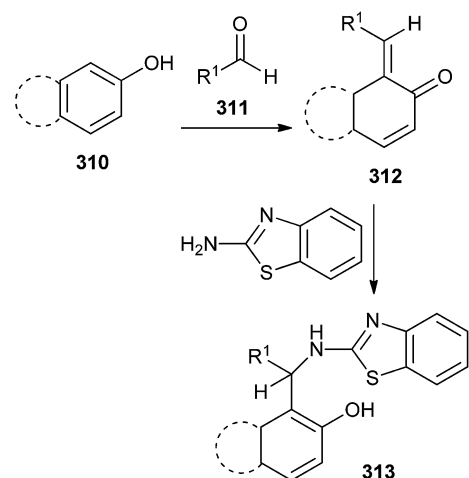
Scheme 62 Bis-bromination of ethano-dimer of  $\alpha$ -tocopherol.Scheme 63 Cyclocondensation reaction via *o*-QMs intermediates.

1,2-Dihydroronaphtho[2,1-*b*]furans and 2,3-dihydrobenzofurans **316** substituted at C-2 by an acyl or aryl group were prepared in a diastereoselective manner. The reaction goes through the formation of the *o*-quinone methide intermediate followed by a Michael-type addition of the ylide **315** to the *o*-QM with a consequent intramolecular nucleophilic substitution. The reaction is applicable to a range of Mannich bases and pyridinium salts with a variety of versatile functional groups (Scheme 67).<sup>66</sup>

Salvadoria and co-workers<sup>67</sup> reported the oxidation of  $\alpha$ -tocopherol **317** leading to *o*-QM species **318**, which when reacted with bromide as a nucleophile from hydrogen bromide, affords the benzylic brominated product **319** (Scheme 68).

Scheme 64 Nucleophilic addition of  $\beta$ -naphthol to aldehyde via *o*-QM intermediacy.

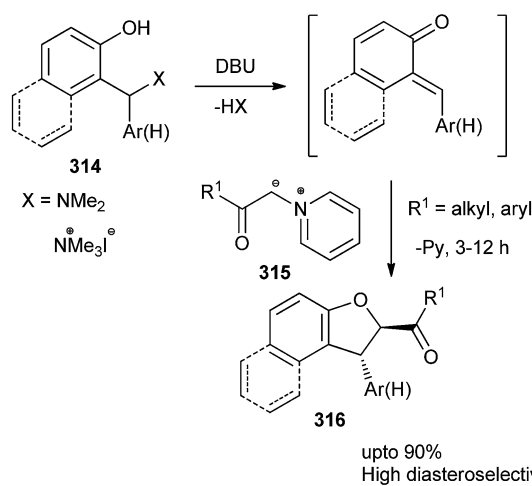
Scheme 65 Synthesis of amidoalkyl naphthols.



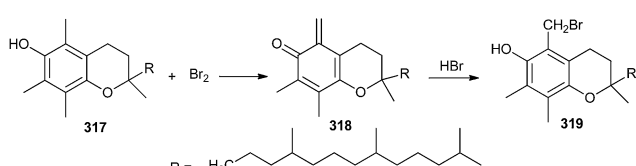
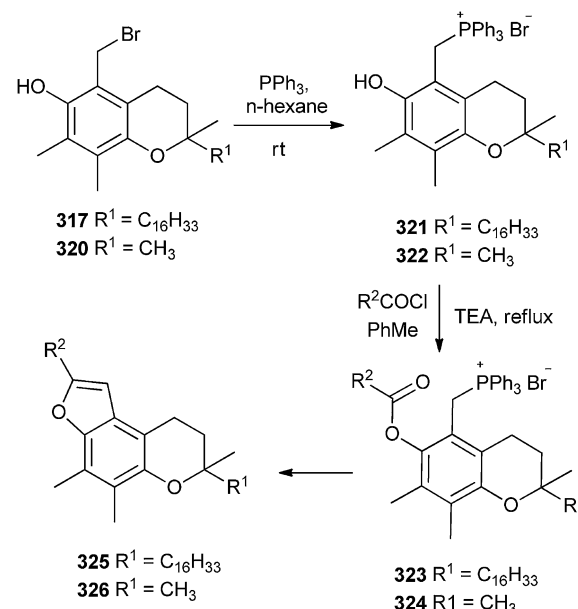
Scheme 66 Synthesis of 2'-aminobenzothiazolomethyl naphthols.

The bromo- $\alpha$ -tocopherols 317 and 320 after treating with nucleophilic triphenyl phosphene followed by acylation gives the furotocooherols 325 & 326 (Scheme 69).<sup>68</sup>

Chen and co-workers<sup>69</sup> reported the stereoselective synthesis of *trans*-dihydrobenzofurans 332 by the reaction of *o*-QM 328 and sulfur ylides 329. This gave intermediate 330, which undergoes *trans*-elimination-cyclization to afford 332. *o*-QM intermediates have been generated from 2-tosylalkylphenols 327 under mild basic conditions (Scheme 70).



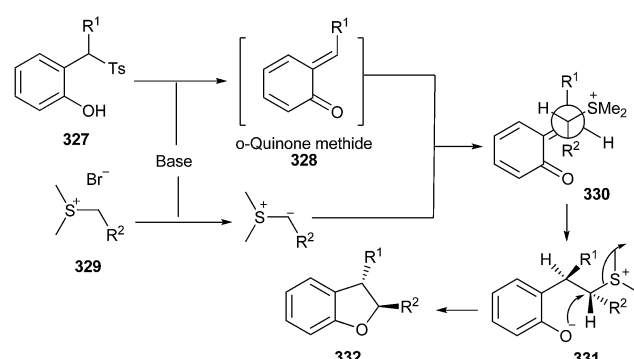
Scheme 67 Diastereoselective synthesis of naphthofurans and benzofurans.

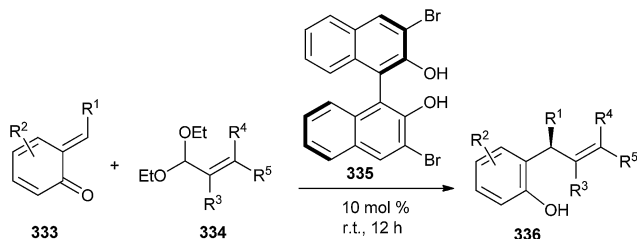
Scheme 68 Bromination of  $\alpha$ -tocopherol.Scheme 69 Synthesis of urotocooherols from bromo- $\alpha$ -tocopherols.

Chiral biphenols were found to catalyze the enantioselective asymmetric addition of aryl- or alkenylboronates to *o*-QMs 333. Thus, substituted 2-styrylphenols 336 were obtained in high yields (up to 95%) with high enantiomeric ratios (up to 98 : 2) in the presence of 10 mol% of 3,3'-Br<sub>2</sub>-BINOL 335 (Scheme 71).<sup>70</sup>

Kumar and co-workers<sup>2,71</sup> have developed an efficient and catalyst-free approach for C-H hydroarylation of *in situ* generated *o*-QM 339 with electron-rich arenes (*tert*-aryl amines 340) in a glycerol medium. A number of 3-substituted 4-hydroxycoumarin 341 and 4-hydroxypyrone derivatives were obtained in good to excellent yields. The reaction takes place in water without any catalyst, and is highly regioselective (Scheme 72). They have used coumarins, indole, and 4-hydroxypyrone derivatives to generate corresponding *o*-QMs. It is noteworthy that in all the cases, *para* substituted products were exclusively obtained. The reason of regioselectivity is the steric hindrance of *N*-alkyl group and *ortho* hydrogen of *N,N*-dialkylanilines, which provides the *para* selectivity.

Antonio and Freccero<sup>72</sup> have reported the synthesis and the unexpected photochemical reactivity of a new class of

Scheme 70 Stereoselective synthesis of *trans*-dihydrobenzofurans.



Scheme 71 Enantioselective addition of aryl- or alkylboronates to *o*-QMs.

naphthalimide derivatives (NIs) 342 bearing quinone methide precursor (QMPs) at the imide moiety by irradiation of the NI core (Scheme 73). Photogeneration of the transient QM 343 through a PET mechanism between the phenolic precursors and the NI core was rationalized. Such reactivity represents the first case of non-direct phototriggering of QMs *via* photoinduced electron transfer (PET) involving a tethered peripheral moiety.

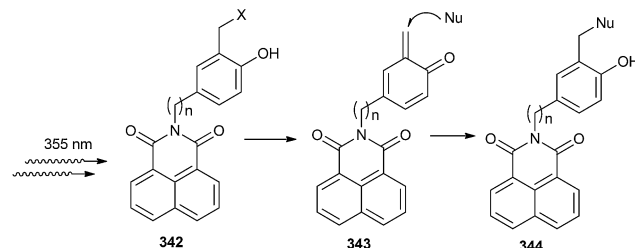
Freccero and co-workers<sup>26</sup> have reported the photoinduced generation of new binol quinone methides 349, which undergo mono- and bisalkylation of free nucleophiles by product distribution analysis and laser flash photolysis in water solution using binol quaternary ammonium derivatives 346 and 352 as photoactivated precursors (Schemes 74 and 75). *N* and *S* nucleophiles are powerfully competitive in alkylation with the hydration reaction.

The DNA cross-linking potency of the water-soluble binol quaternary ammonium salt 346 was investigated as a pH function and compared to that of other quaternary ammonium salts proficient for photogenerated benzo-QM by gel electrophoresis. DFT calculations in the gas phase and in water bulk on the binol and benzo quaternary ammonium salts 346 and 352 evidence structural and electrostatic features of the binol derivative, which might offer a validation of its promising high photo-cross-linking efficiency.

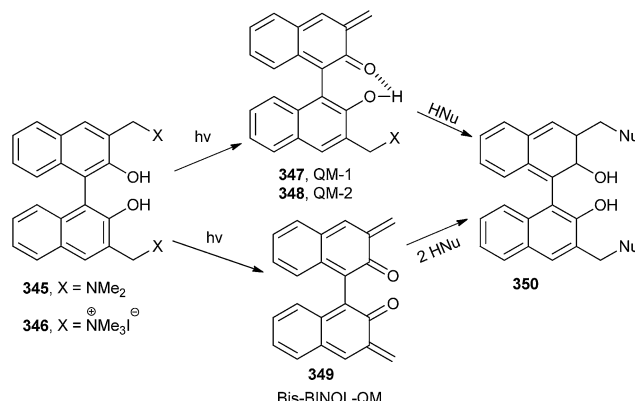
*o*-QM 358 (NDI-QM) has been generated by activation of suitable quinone methide precursors (QMPs) 357 under biocompatible conditions such as mild thermal digestion (40 °C), UV-Vis irradiation and mild mono-electronic reduction (Scheme 76).<sup>73</sup> The conjugated NDI-QMPs might have been acting as a hybrid ligand-alkylating structures selectively targeting G-4 folding oligonucleotides.

### 3.3. Alkylation on *o*-QM: DNA alkylation

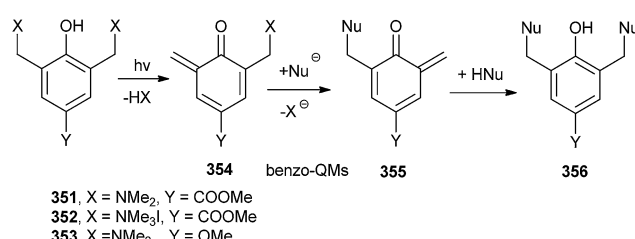
The formation of QMs depends on the strength of the leaving group attached to the benzylic position of *o*-QM 360 in the



Scheme 73 Phototriggering of QMs *via* photoinduced electron transfer (PET).

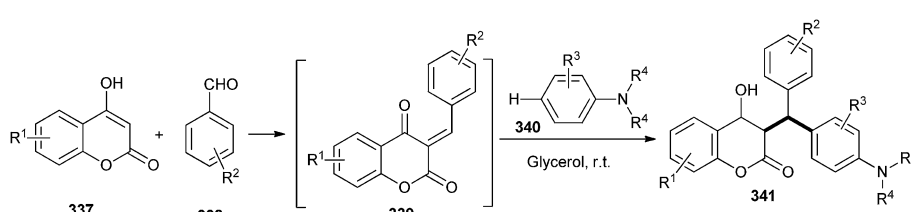


Scheme 74 Addition of nucleophiles on binol quinone methides.

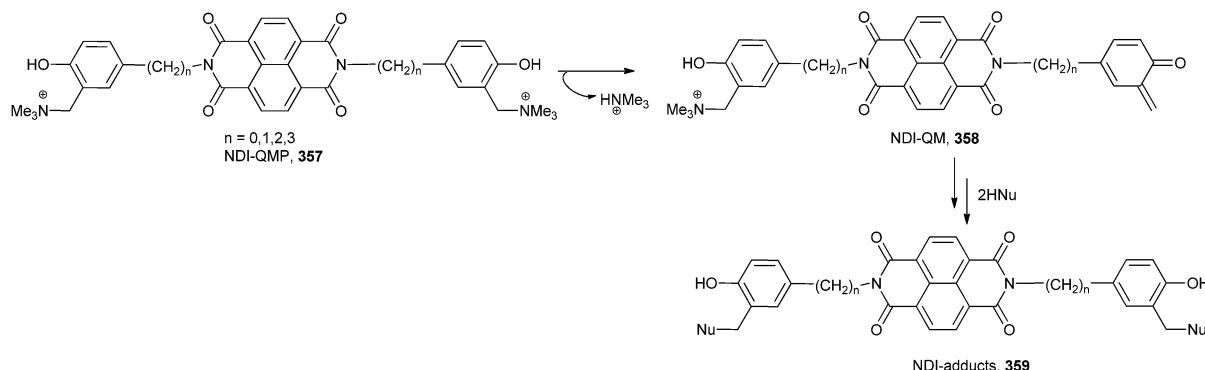


Scheme 75 Bis-alkylation of photoinduced *o*-QM 354 and 355.

presence of biological nucleophiles (dN).<sup>74,75</sup> The formation and reaction of QMs are also highly responsive to the presence of electron-withdrawing and electron-donating groups. The observed trends of reactivity are consistent with the electron-deficient nature of the QM intermediate. Electron-donating groups greatly facilitate initial QM generation and its subsequent regeneration from adducts formed by the nucleophiles of



Scheme 72 C-H hydroarylation of *in situ* generated *o*-QM.



Scheme 76 Addition of nucleophile on NDI-QM 358.

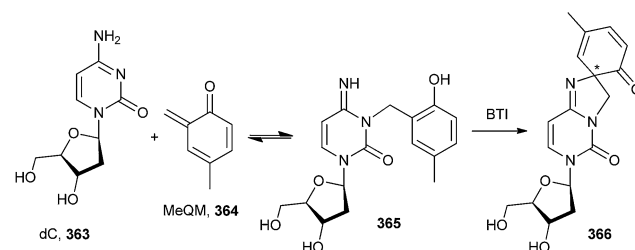
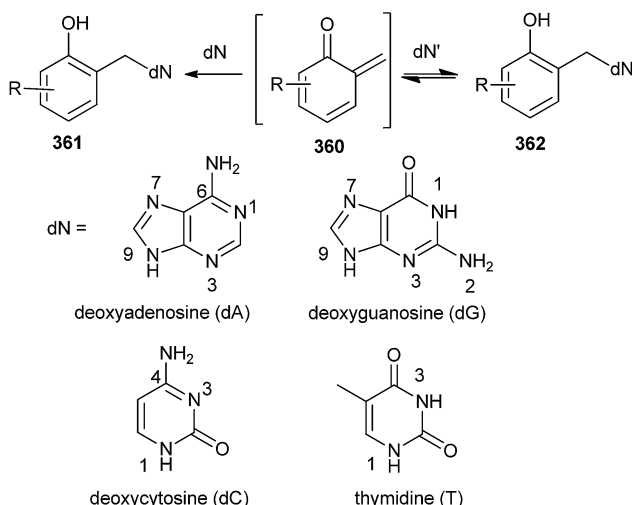
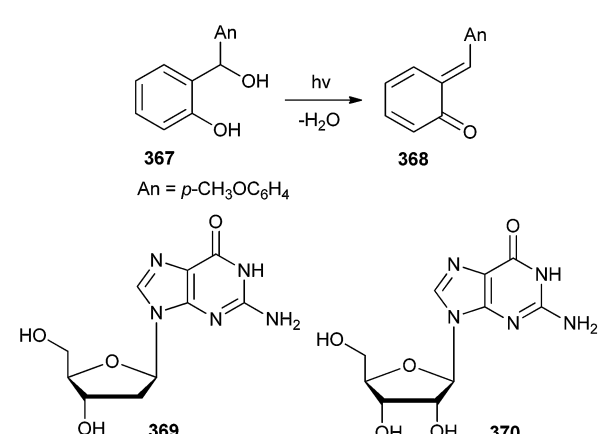
deoxynucleosides (dN) that also function as good leaving groups. Conversely, electron-withdrawing groups greatly suppress initial formation of QM and its regeneration from the reversible deoxynucleoside adducts 362 (Scheme 77). The stability of *o*-QM is mainly influenced by the electronic perturbation over it, and the kinetics of the product formation is also altered by the reaction with deoxynucleosides.<sup>76</sup> Electron-rich QMs react considerably more slowly but selectively with nucleophiles than the electron-poor QMs. These fundamental characteristics provide the basis for explaining the product profiles observed after DNA has been exposed to various QMs.<sup>77</sup> These characteristics are used to fine-tune the stability and reactivity of QM conjugates for target-promoted and gene-specific alkylation.<sup>78</sup>

Rokita and co-workers<sup>79</sup> reported the formation of the reversible quenching adducts 366 under physiological conditions between *o*-QM 364 and deoxycytidine 363 by selective oxidation using bis[(trifluoroacetoxy)iodo]benzene (BTI), which induces a surprising rearrangement driven by over oxidation of a derivative lacking an alkyl substituent at the 4-position of the QM (Scheme 78).

The rates of alkylation of 2'-deoxyguanosine 369 and guanosine 370 with *o*-quinone  $\alpha$ -(*p*-anisyl)methide 368

(Scheme 79) were studied by flash photolysis in a series of aqueous sodium hydroxide solutions and bicarbonate ion, *t*-butylhydrogenphosphonate ion as well as in biphosphate ion buffers.<sup>80</sup> Rate constants showed the reaction of *o*-quinone  $\alpha$ -(*p*-anisyl)methide 368 with guanosine and deoxyguanosine to be quite a fast process. Even it was considerably faster than the biologically wasteful reaction of the quinone methide with water, which is the ubiquitous medium in biological systems, and hence makes the quinone methide a potent guanosine and deoxyguanosine alkylator.

The selenide derivatives 371 can generate covalent inter-strand cross-linking with its complementary strand through the

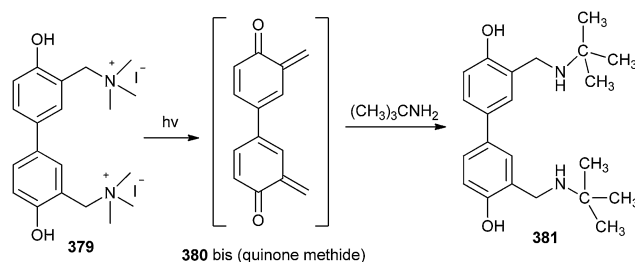
Scheme 78 Reaction of *o*-QM with deoxycytidine 363.Scheme 77 Generation of deoxynucleoside and *o*-QM adducts.Scheme 79 Alkylation of 2'-deoxyguanosine and guanosine on *o*-quinone  $\alpha$ -(*p*-anisyl)methide.

formation of *o*-QM intermediate 373, induced by periodate oxidation.<sup>81</sup> It has been evidenced by hydroxyl radical footprinting experiments that the quinone appendage specifically alkylated the cytosine base (nuc) extending the duplex formed between the conjugate and the target strand (Scheme 80).

It is well known that cation on porphyrin can increase both selective binding affinity to nucleic acid or protein and solubility in aqueous conditions. Hence, with photoinducing, *o*-QM intermediate and singlet oxygen could be formed and they may play an important role for both alkylation and oxidative damage to nucleic acids or proteins. In all probability, porphyrin 377 was photochemically activated and induced to form both singlet oxygen and *o*-QM intermediate 378, which led to both oxidative damage and the alkylation of the organism in the bacterial system (Scheme 81).<sup>82</sup>

Song and co-workers<sup>83</sup> reported three water-soluble DNA cross-linking phenol quaternary ammonium derivatives, which could inhibit the transcription *in vitro* by photo-activation. The cross-linking agent 379 could be a significant reason for the late apoptosis of tumour cells. The twisted form and two quaternary ammonium groups could anchor DNA strands and facilitate the binding of DNA strands and the cross-linking between strands can then proceed through a bis(quinone methide) intermediate 380. The *in situ* formed *o*-QM has also been trapped by *t*-BuNH<sub>2</sub> (Scheme 82).

Quinolinyl QM 387 was designed through the fluoride-induced QM generation by desilylation and elimination of acetate group from compound 386 (Scheme 83). The incorporation of the quinolinyl substitute was designed to enhance the potential interactions with DNA through possible partial intercalation and charges of the quinoline moiety and also for the investigation of the steric effect on the reactivity of QMs.



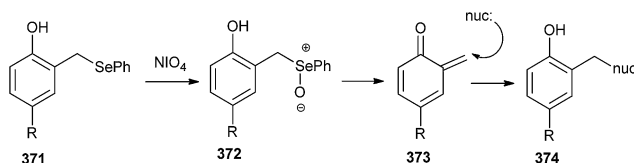
Scheme 82 Trapping of bis(quinone methide) intermediate by *t*-BuNH<sub>2</sub>.

Authors have reported that the N1-dG adduct 388 was selectively formed with quinolinyl QM as a favored dG adduct in 30% aqueous DMF and 10 mM phosphate buffer (pH 7.0).<sup>84</sup>

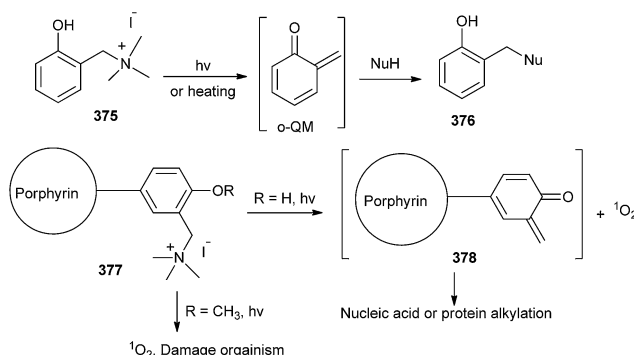
A novel G-quadruplex (G-4), ligand/alkylating hybrid structures 391 tethering the naphthalene diimide moieties to quaternary ammonium salts of Mannich bases, as quinone-methide precursors 389, was activated by mild thermal digestion (40 °C).<sup>85</sup> The bis-substituted naphthalene diimides were capably synthesized and their reactivity as activatable bis-alkylating agents was explored in the presence of thiols and amines in aqueous buffered solutions (Scheme 84). During alkylation, it has been found that the reversible process is a precondition to DNA alkylation, which in turn strengthens the G-quadruplex structural reorganization.

Freccero and co-workers<sup>86</sup> also reported a photoactivation of new BINOL-amino acid and BINOL-amino ester conjugates acquiesced alkylating and DNA cross-linking agents with high photoefficiency and superior cytotoxicity. While using nucleosides as nucleophiles, only the conjugate adducts with deoxy-cytidine at the N3 (dC-N3), deoxyadenosine at both N1 and NH<sub>2</sub> (dA-N1 and dA-NH<sub>2</sub>), and deoxyguanosine at NH<sub>2</sub> (dG-NH<sub>2</sub>) are stable in water solution. Conversely, the alkylation adducts at N7 of both dG and dA are thermodynamically unstable, because the reversal of the alkylation becomes a competitive process.

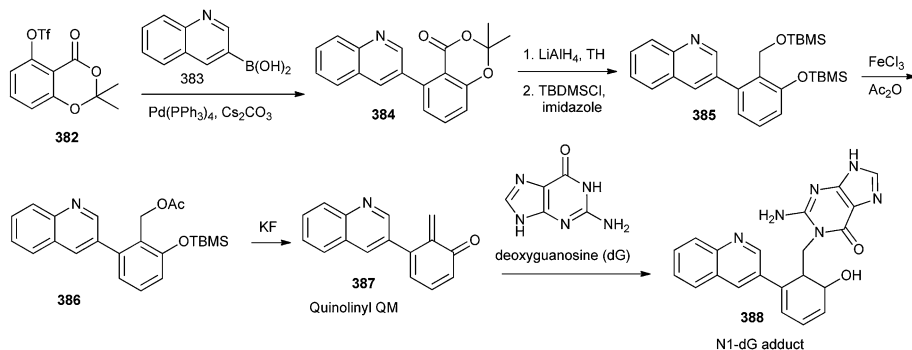
The alkylation reaction of 9-methyladenine and 9-methylguanine (as prototype substrates of deoxyadenosine and deoxyguanosine) with the parent *o*-QM have been studied by using DFT at the B3LYP/6-311+G(d,p) level.<sup>87</sup> The guanine oxygen atom ( $O^6$ ) ( $\Delta G_q$  gas, 5.6 kcal mol<sup>-1</sup>) followed by the adenine N1 ( $\Delta G_q$  gas, 10.3 kcal mol<sup>-1</sup>) are more nucleophilic, whereas other centres have comparatively lower nucleophilicity. But water as a solvent diminishes the nucleophilicity of both 9-methyladenine N1 ( $\Delta G_q$  solv, 14.5 kcal mol<sup>-1</sup>) and 9-methylguanine O6 ( $\Delta G_q$  solv, 17.0 kcal mol<sup>-1</sup>), and as a consequence it reverts the purine base nucleophilicity. Regarding the product stability, calculations predict that only two adducts of *o*-QM with 9-methyladenine at NH<sub>2</sub> and N1 positions, are in lower energy than reactants, in the gas and water phases. However, adduct at N1 can easily be dissociated in water. In particular, the oxygen alkylation adduct becomes slightly unstable in water ( $\Delta G_{solv}$ , +1.4 kcal mol<sup>-1</sup>), and the N7 alkylation product remains only moderately more stable than free reactants ( $\Delta G_{solv}$ , -2.8 kcal mol<sup>-1</sup>).



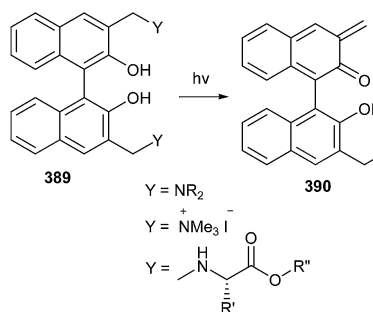
Scheme 80 Alkylation of *o*-QM by using cytosine base (nuc).



Scheme 81 Binding of nucleic acid or protein on *o*-QM having porphyrin unit.



Scheme 83 Synthesis of N1-dG adduct using quinolinyl QM and deoxyguanosine.

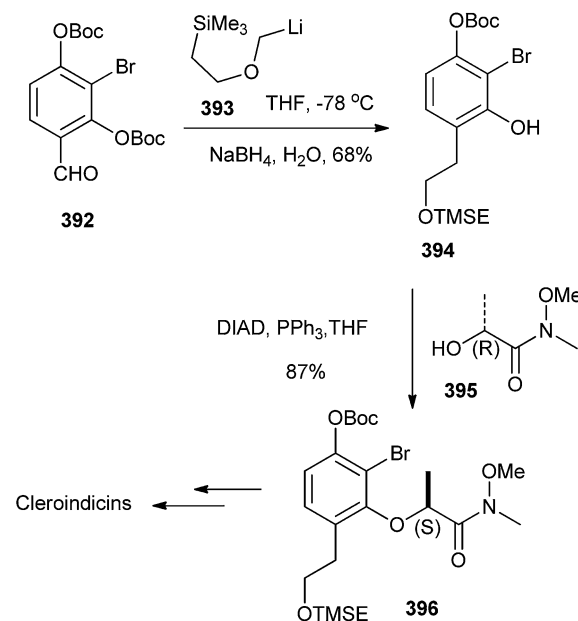
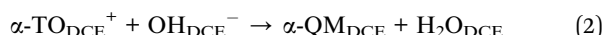
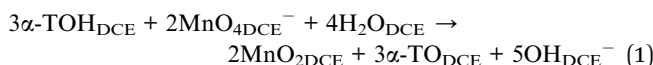


Scheme 84 DNA alkylation o-QM precursors to generate G-quadruplex.

Pettus *et al.*<sup>88</sup> have reported the total synthesis of all of the known chiral Cleroindicins from the known substituted benzaldehyde 392, which has been treated with [(2-(trimethylsilyl)ethoxy)methyl]lithium 393 resulted in Boc migration, and afforded an intermediate phenoxide. This phenoxide generated the *o*-QM by *in situ* elimination, which then underwent succeeding *in situ* 1,4-reduction with sodium borohydride to produce the phenol 394 in a 68% yield. Mitsunobu coupling of compound 394 with amide 395 afforded the inverted amide 396 in an 85% yield and >99% ee (Scheme 85).

#### 3.4. Coupling reactions

The coupling of *o*-QM has been done by redox reactions of vitamin E in 1,2-dichloroethane with oxidants in water/1,2-dichloroethane interface.<sup>89</sup> Here, the oxidation reaction of  $\alpha$ -tocopherol (TOH) with  $MnO_4^-$  in DCE has been explained by a series of reactions (eqn (1)–(3)). After the formation of  $\alpha$ -TD in hexane and *o*-QM of  $\alpha$ -TOH produced during the oxidation of  $\alpha$ -TOH dimerizes easily to  $\alpha$ -TD, as shown in Scheme 86.

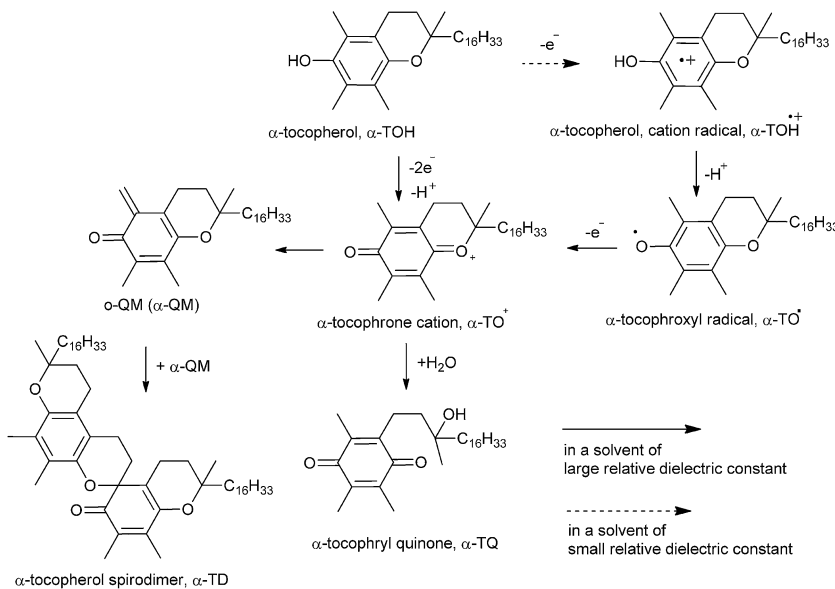
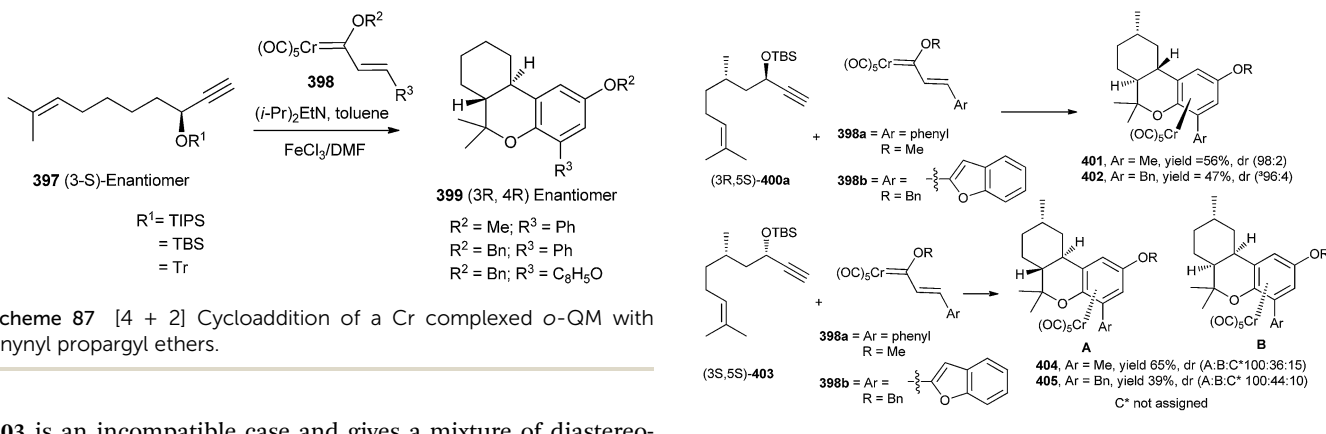


Scheme 85 Synthesis of chiral Cleroindicins from the substituted benzaldehyde 392.

#### 3.5. Complex formation with metals

Korthals and Wulff<sup>90</sup> reported that the reactions of Chromium carbene complexes of type 398 with enynyl propargyl ethers 397 in the presence of a base would generate hexahydrodibenzopyrans 399 after an oxidative workup. The involvement of a [4 + 2] cycloaddition of a Cr complexed *o*-QM intermediate was inferred from the observed high asymmetric induction (Scheme 87).

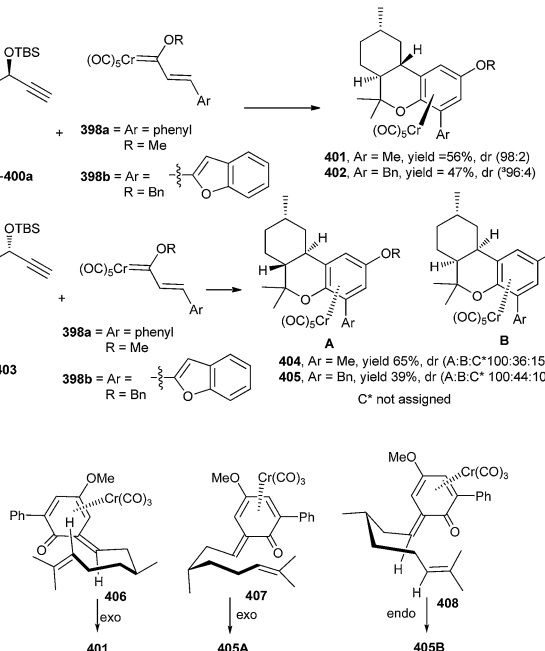
Compound 401 was prepared through the Diels–Alder reaction of the *o*-QM intermediate 406. The methyl group at the C-9 position of *o*-QM 406 puts into effect the formation of a single diastereomer from the Diels–Alder reaction possessing a chair transition state in an *exo*-cycloaddition where the  $CH_3$  is in an equatorial position. Such a chair transition state is possible in 406, where the cycloaddition occurs *anti* to the chromium. But in the case of diastereomer 407, the Cr is on the opposite face of the *o*-QM, where the chair transition state for the *exo*-cycloaddition *anti* to the metal has an axial methyl. The (3*S*,5*S*)-enye

Scheme 86 Formation and dimerization of  $\alpha$ -TD.Scheme 87 [4 + 2] Cycloaddition of a Cr complexed  $\alpha$ -QM with enynyl propargyl ethers.

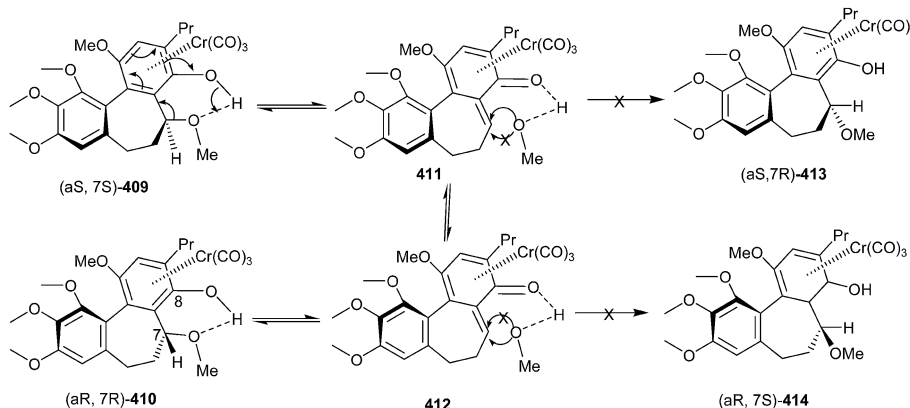
**403** is an incompatible case and gives a mixture of diastereomers, the two most predominate of which are formed *via* an *exo*-cycloaddition with a chair transition state with an axial methyl **407** and an *endo*-cycloaddition with a chair transition state with an equatorial methyl **408** (Scheme 88).

Wulff and co-workers<sup>91</sup> also disclosed the synthesis of allocolchicinoids that involves the benzannulation reaction of the Fischer chromium carbene complexes and alkynes with high to moderate diastereoselectivity. One of the diastereomer **409** was recemicized, but not the other **413**. The intermediacy of an  $\alpha$ -quinone methide chromium tricarbonyl complexes **411** & **412** and the intramolecular hydrogen bonding assist the reversible dissociation of methanol in compound (aS, 7S) **409** to give (aR, 7R) **410**. Due to the intramolecular H-bonding, it only becomes possible in diastereomer **409**, whereas the opposite diastereomer **413** would not participate, and thus retains its enantiomeric purity (Scheme 89).

QMs could be stabilized by the steric bulk or by coordination to electron-rich transition metal complexes. The mechanism of an enantioselective palladium-catalyzed alkene difunctionalization reaction gives evidence of rapid ligand exchange between palladium and copper, as well as a

Scheme 88 Diastereoselective synthesis of hexahydrodibenzopyrans *via* a chair transition state of a Cr complexed  $\alpha$ -QM.

correlation between ligand electronic nature and enantioselectivity.<sup>92</sup> A substrate having an alkene with an adjacent *ortho*-phenol and a linked nucleophile **415** was used. *ortho*-Phenol not only coordinates the Pd(II) intermediate **416**, preventing hydride elimination, but it also allows for the *in situ* formation of an electrophilic quinone methide **418**, necessary for the second functionalization (Scheme 90). So this approach contrasts with others in the oxidation of the substrate, because the Pd centre does not promote the addition of the second nucleophile.



Scheme 89 Synthesis of alallocolchicinoids involving Fischer chromium carbene complex and alkynes.

Pd(II) catalyzes the aerobic reductive coupling reactions of organometallic reagents and styrenes through *o*-QM intermediates.<sup>93</sup> Compound A initially oxidizes the alcoholic solvent to generate the Pd-hydride intermediate B, which coordinates with alkene 419 to give cationic complex C. The alkene inserts into the Pd-hydride yielding D and D'. As the consequence of formation of the benzylic addition product only, it has been emphasized that intermediate D' proceeds to product *via* formation of *o*-QM E, with concomitant reduction of Pd(II) to Pd(0) and generation of 420. Subsequently, ethanol reacts with the *o*-QM E to liberate the ether product 420 and the Pd(0) F, which has been reoxidized by CuCl<sub>2</sub> or O<sub>2</sub> (Scheme 91).

Phenols when bound to pentaammine osmium(II) 424, readily react with aldehydes 425 to generate the complexes of *o*-QMs 427. While these complexes are remarkably stable, when exposed to air or dissolved in water, treatment with CAN oxidizes the metal and releases the intact QM ligand, which can be trapped by a suitable dienophile 428 to give the compound 429 (Scheme 92).<sup>94</sup>

Whenever the phenol complex was treated with acetaldehyde, it gave the *o*-QM 430 with small amounts of acetaldehyde complex [Os(NH<sub>3</sub>)<sub>5</sub>(acetaldehyde)]<sup>2+</sup>. The reaction of complex 430 with an

excess of 3,4-dihydropyran and 1.5 equiv of CAN in acetonitrile provided tetrahydropyranochromene 431 (Scheme 93).

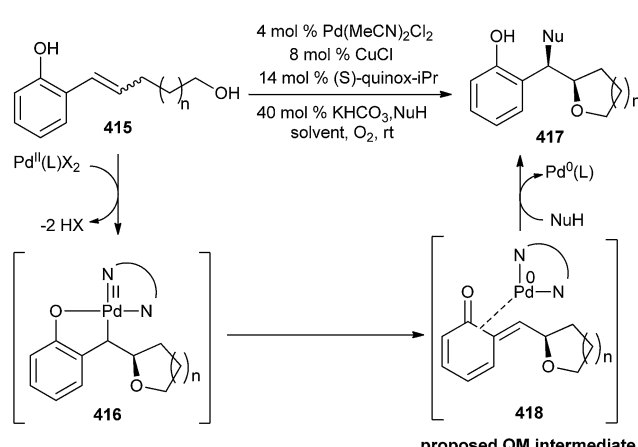
The intramolecular Diels–Alder reaction was accomplished by using the *o*-QM 432, which was formed by treatment of the phenol complex 424 with (R)-citronellal and pyridine. Compound 432, after treatment with CAN, leads to the demetallation and cycloaddition to form the benzo[c]chromene 433 in 52% yield as a single diastereomer (Scheme 94).

Cycloaddition reactions of activated olefins and styrenes 435 with *o*-quinine methides 436 in the presence of PtCl<sub>4</sub> and AuCl<sub>3</sub> gave a wide range of 2-alkyl or 2-aryl chromans 437. Good diastereoselectivity (up to >99 : 1) of the chromans was obtained (Scheme 95).<sup>95</sup>

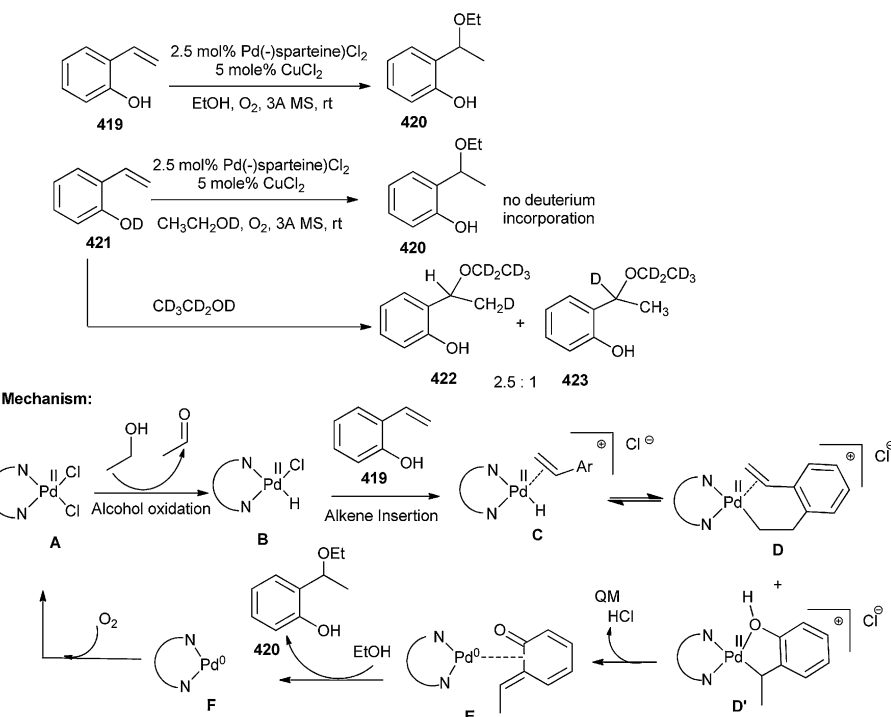
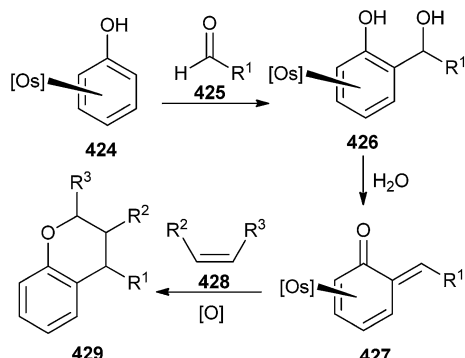
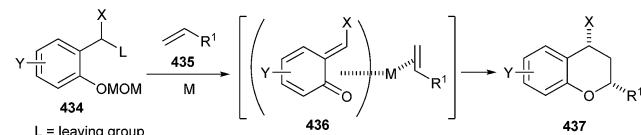
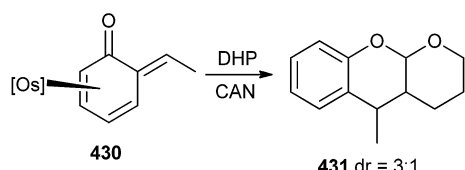
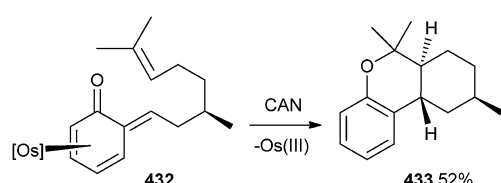
The reactivity<sup>96</sup> of an *o*-QM can be understood from M<sup>III</sup> resonance form in which the carbon can be viewed as bearing a negative charge (Scheme 96). It has been emphasized that the stabilisation of *o*-QM could be correlated to the degree of deviation of the carbonyl/alkene segment of the *o*-QM from planarity with the coordinated diene segment, which is a consequence of metal back-bonding into the aromatic system.

Metal stabilised *o*-QM showed a complete reverse effect; the methylene carbon became nucleophilic upon transition metal coordination. For example, in Cp<sup>\*</sup>Ir(*o*-QM) 442 the exocyclic carbon undergoes nucleophilic substitution reactions, *e.g.* with iodine or methyl propiolate, and [3 + 2] dipolar cycloadditions, as in the case of the electron-poor dienophile N-methylmaleimide 443 (Scheme 97). The partial charge and hinge angle follow the order Ru < Co < Rh < Ir. The Ru and Co complexes predicted high reactivity. Mono substituted nucleophilic metal complexes were isolated to establish the importance to the application of this chemistry for the stereoselective synthesis.

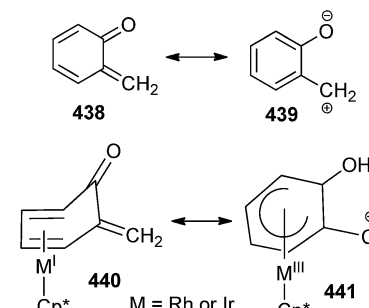
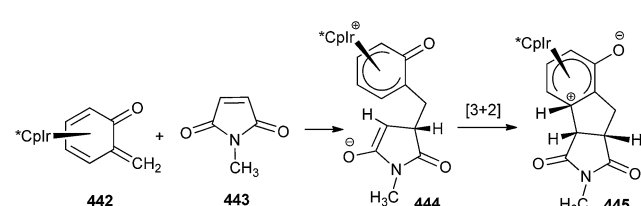
Knoevenagel reaction of 2-hydroxy-1,4-naphthoquinone, 4-hydroxycoumarin, and 4-hydroxy-6-methylcoumarin with paraformaldehyde generated respective quinone methides 447, 448 and 449. They applied these *in situ* generated intermediate in the hetero-Diels–Alder reaction with  $\beta$ -vinyl-*meso* tetraphenylporphyrinatozinc(II) 446, leading to macrocycles containing 5,10-dioxobenzo[g]chromene, 5,6-dioxobenzo[h]chromene 450, pyrano[3,2-*c*]coumarin 451, and benzopyran 452 motifs at the  $\beta$ -position (Scheme 98).<sup>97</sup>

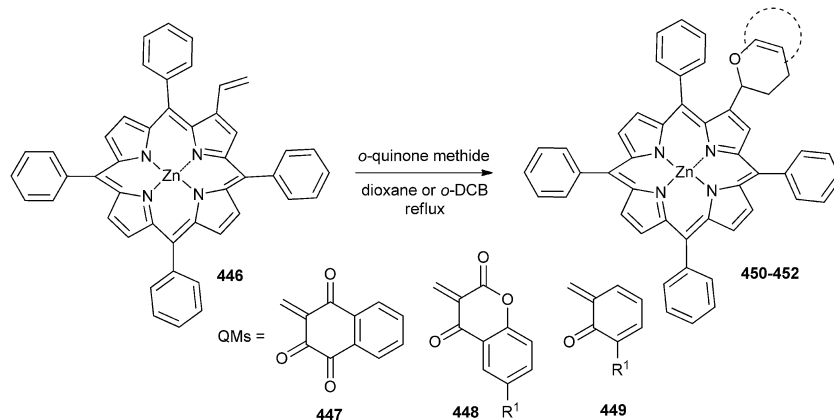


Scheme 90 Enantioselective palladium-catalyzed difunctionalization of alkene.

Scheme 91 Pd(II) catalyzed reductive coupling of organometallic reagents and styrenes via *o*-QM intermediate.Scheme 92 Trapping of Os-complexed *o*-QM by different alkenes.Scheme 95 Cycloaddition reactions of activated olefins with *o*-QM.Scheme 93 Reaction of Os-complexed *o*-QM with 3,4-dihydropyran.

Scheme 94 Diastereoselective synthesis of benzo[c]chromene.

Scheme 96 Resonating forms of metal *o*-QM complex.Scheme 97 Cycloaddition reaction of *Cp*\*Ir(*o*-QM) with *N*-methylmaleimide.

Scheme 98 Hetero-Diels–Alder reaction of *o*-OMs with  $\beta$ -vinyl-*meso* tetraphenylporphyrinatozinc(II).

### 3.6. Rearrangement reactions

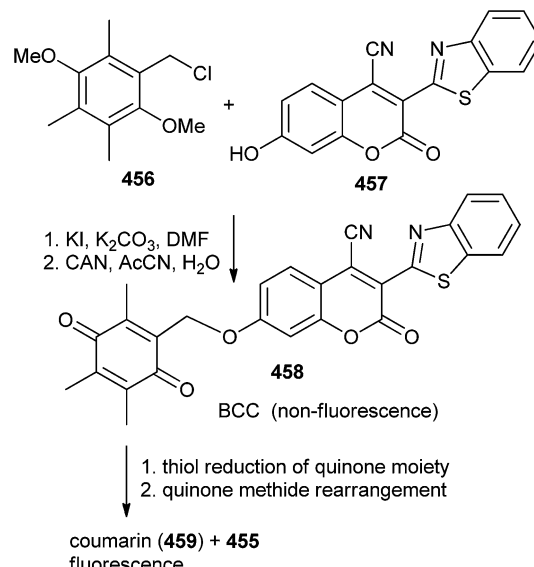
The chemical transformation of fluorogenic BCC triggered by thiols proceeds through a tandem benzoquinone reduction and QM type rearrangement reactions, which are spontaneous and irreversible at physiological temperatures in aqueous media.<sup>98</sup> In general, the intracellular reduction of the quinone moiety 453 produces the corresponding hydroquinone 454 that instinctively releases the deactivated drug and gives compound 455 *via* a QM-type rearrangement (Scheme 99).

QM-type rearrangement reaction sequence has been employed as part of the fluorescence releasing mechanism for latent fluorophores or the drugs release mechanism of the prodrugs, as shown in Scheme 100.

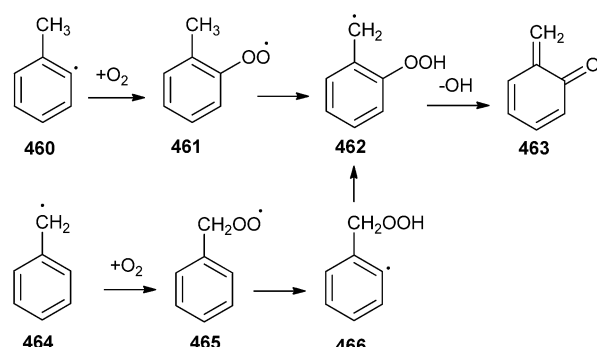
Silva and Bozzelli<sup>99</sup> have reported that *o*-QM, a 6-methylene-2,4-cyclohexadiene-1-one is an important intermediate in lignin and alkyl benzene combustion, and so the thermal decomposition of *o*-QM is pertinent to the combustion of transportation fuels (containing toluene) and of biomass and low-rank coals (containing lignin). A potential pathway leading to *o*-QM 463 formation has been demonstrated by the reaction of the benzyl radical 464 with  $O_2$ , which would also be important in toluene combustion (Scheme 101).

The formation of tropone *via* a hydroxyphenylcarbene intermediate 467 from *o*-QM undergoes an intramolecular hydrogen shift to produce 2-hydroxyphenylcarbene 467 in a concerted process (Scheme 102).

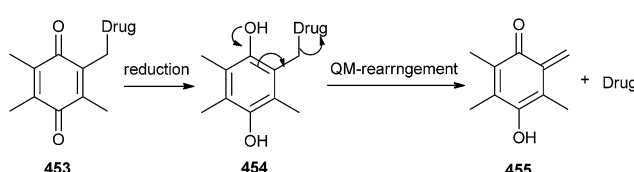
Eventually, the mechanism for fulvene (+CO) formation has been considered. The ring opened product 470 cyclises to the bicyclic intermediate bicyclo[3.2.0]hepta-3,5-dien-1-one 471, which rearranges to yield spiro[2.4]hepta-4,6-dien-1-one (472).



Scheme 100 Drugs release mechanism of the prodrugs.



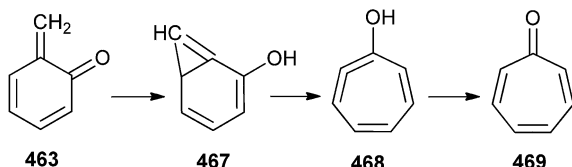
Scheme 101 Combustion of toluene.



Scheme 99 Generation of deactivated drug via QM-type rearrangement.

This intermediate subsequently dissociates to fulvene 473 and CO (Scheme 103).

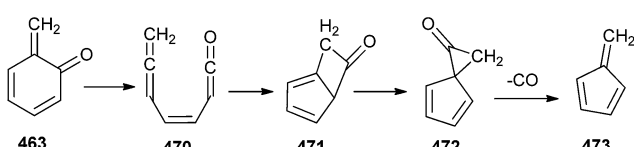
It has been assumed<sup>100</sup> that the structure obtained after proton transfer is a resonance hybrid of two possible forms,

Scheme 102 Synthesis of tropone from *o*-QM.

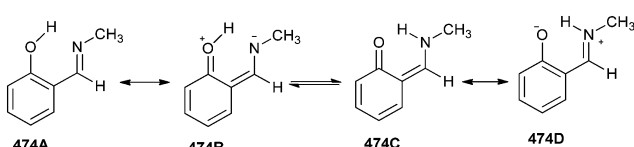
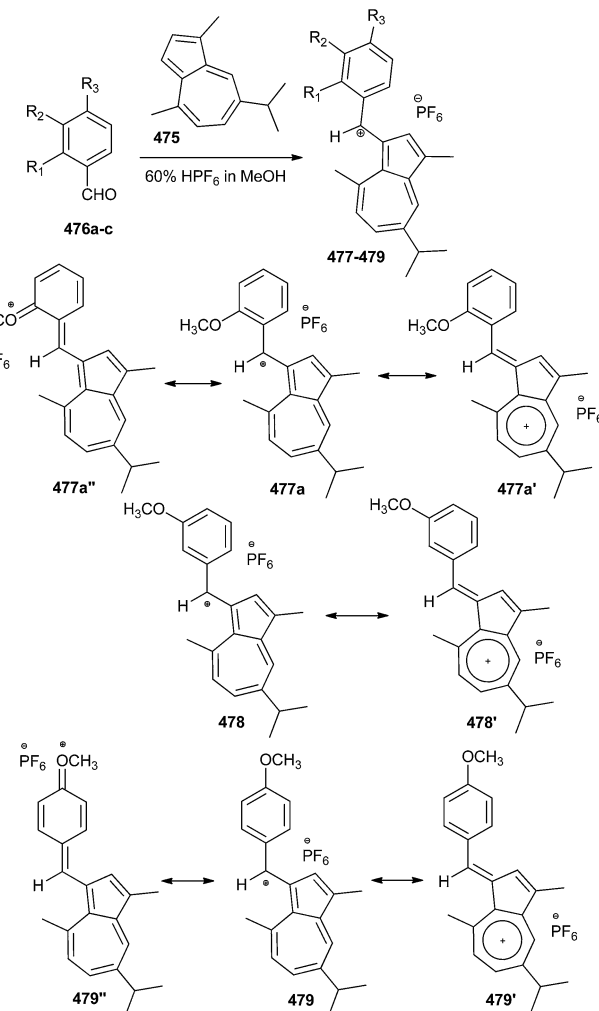
zwitterionic (*ortho*-quinoid, **474B**) and keto enes (*ortho*-quinoid, **474C**), as shown in Scheme 104. The wave function of the real structure is a linear combination of the wave functions of two resonance forms. The results demonstrate that not only resonance enhances the strength of hydrogen bonds, but also that the formation of intramolecular hydrogen bonds leads to more efficient resonance. The value of this stabilization can be estimated as a difference in energy between the proton transfer state and the open one, which is about 5 kcal mol<sup>-1</sup> in *N*-methyl-2-hydroxybenzylideneamine.

Reaction of guaiazulene<sup>101</sup> **475** with 2-methoxybenzaldehyde **476** in methanol in the presence of hexafluorophosphoric acid at 25 °C gives (3-guaiazulenyl)(2-methoxyphenyl)methylium hexafluorophosphate **477** with 93% yield. Similarly, reaction of **475** with 3-methoxybenzaldehyde under the same reaction conditions affords (3-guaiazulenyl)(3-methoxyphenyl)methylium hexafluorophosphate **478** (91% yield) or with 4-methoxybenzaldehyde gives (3-guaiazulenyl)(4-methoxyphenyl)methylium hexafluorophosphate **479** (97% yield). The crystal structures of these monocarbenium-ion compounds, possessing interesting resonance forms, are stabilized by the 3-guaiazulenyl and anisyl (2-, 3-, or 4-methoxyphenyl) groups (Scheme 105).

The regiochemical product of Pictet–Spengler cyclization reactions, focussed toward the preparation of the pentacyclic core of the ecteinascidin class of antitumor antibiotics, has been explored on two different phenolic substrates.<sup>102</sup> The reduction of the β-lactam unit in compound **480** proceeds through the coordinated lithium complex **481**, which also prevents the over-reduction of the corresponding aldehyde group. Following aqueous quench with NH<sub>4</sub>Cl, condensation of



Scheme 103 Synthesis of fulvene.

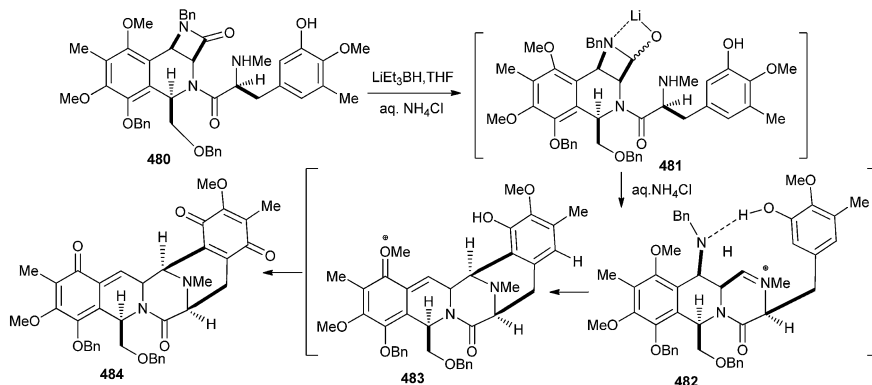
Scheme 104 Resonating structures of zwitterions (*ortho*-quinoid, and keto enes).Scheme 105 Reaction of guaiazulene with methoxybenzaldehyde and resonating structure of products **477–479**.

the secondary amine group onto the hemi-aminal unit **481** led to the key iminium ion intermediate **482**. The expected hydrogen bonding between the C-4 benzylic amine and the E-ring phenolic residue directs the Pictet–Spengler cyclization *ortho* to the phenol. Finally, spontaneous elimination of the C-4 benzylamine group occurs through the intermediacy of *o*-QM **483** to afford the C3–C4 unsaturated pentacyclic compound **484** as the major product (Scheme 106).

### 3.7. Tautomerism

After oxidation, quercetin **485** exists in the four tautomeric forms **486–489**, one *o*-quinone isomer **486** and three quinone methide isomers **487**, **488** and **489**.<sup>103</sup> Due to the relatively high abundance of the quinone methide isomers, glutathionyl adduct formation occurs at positions C6 and C8 of the quercetin A ring to give 6-GSQ **490** and 8-GSQ **491** (Scheme 107).

Depending on the orientation of the indole rings around the single bond, it has been predicted that the pairs of *syn*-periplanar (sp) and *anti*-periplanar (ap) rotamers for the *o*-quinone, quinone methide, and quinonimine tautomers of dimers **493–**

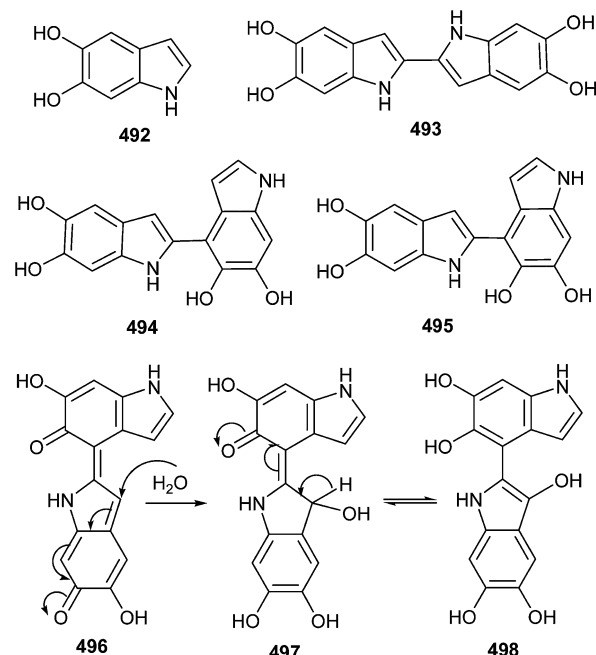


Scheme 106 Pictet-Spengler cyclization reaction for the synthesis of C3-C4 unsaturated pentacyclic compound 484.

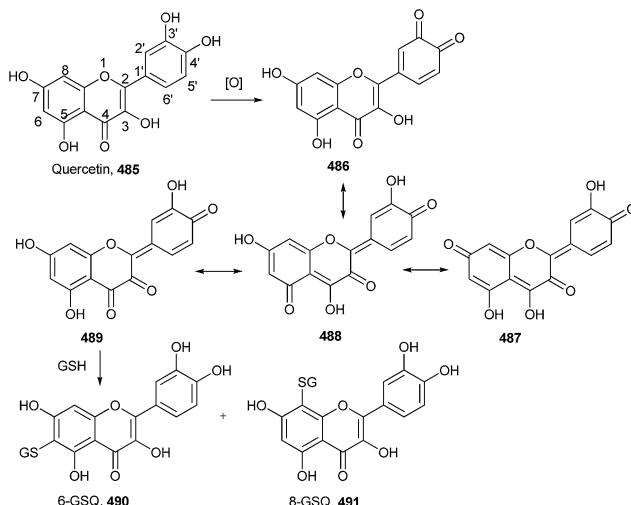
495, two geometrical isomers (*E* and *Z*) are possible for the extended forms.<sup>104</sup> In order to resolve a reasonable entrant among these structures for the observed two-electron oxidation products of the dimers, all tautomeric quinones of dimers 493–495 were geometry-optimized in vacuum at the PBE 0/6-31+G(d,p) level of theory. The pentahydroxybiindolyl 498 was isolated from unprecedented hydroxylated indole derivative by oxidation of dimer 494 (Scheme 108).

Pestacins occur naturally as a racemic mixture of (*S*) 499 and (*R*) 501 enantiomers.<sup>105</sup> This racemization probably occurs post-biosynthetically as enzyme mediated reactions with stereospecificity. A racemization mechanism proceeds through a cationic intermediate 500, which has the desirable feature of being stabilized by different resonating structures. These intermediates are further stabilized by their ability to tautomerize into the three neutral *o*-QMs 501–503 (Scheme 109).

It has been identified that certain aryl quinones experience a tautomeric isomerization to an intermediate QM because of the low barriers of rotation about central aryl-quinone C–C bond, which brings significant implications to consider in the design of synthetic routes leading to natural aryl quinones such as



Scheme 108 Structures of dimers of indole and hydroxybiindolyl.

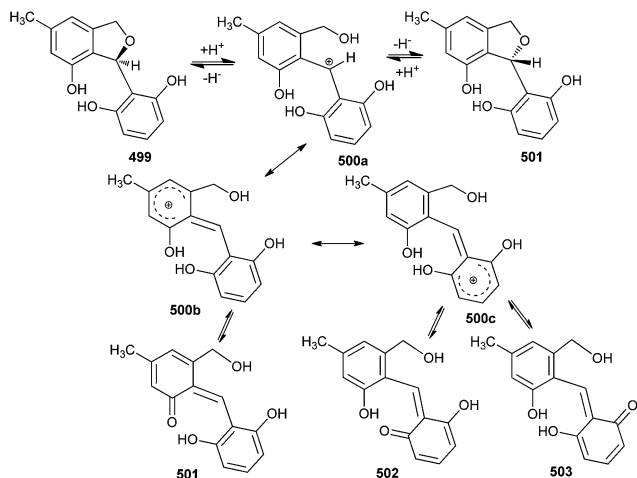


Scheme 107 Glutathionyl adduct formation at the quercetin ring.

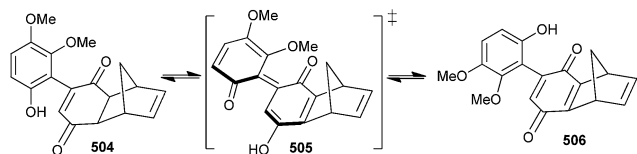
hibarimicin B.<sup>106</sup> The rotational barrier of phenol is significantly lowered due to the stabilization of the transition state structure, leading to the interconversion of 504 and 506 by tautomerization to intermediate QM 505 (Scheme 110).

### 3.8. Photochemical reactions

The photochemistry of a number of *p*-biphenyls and terphenyls substituted with hydroxyl and hydroxymethyl groups in aqueous solutions has been studied in detail by Wan and co-workers.<sup>107</sup> They reported that the simple hydroxyl group can strongly and appropriately activate substituted benzenes or biphenyls towards dehydroxylation due to its strongly electron-donating nature, as well as for being carrier of an acidic proton. The intermediates formed are the corresponding quinone methides (QMs) or biphenyl quinone methides (BQM, 508 & 511), as shown in Scheme 111.



Scheme 109 Resonating structures of Pestacin.

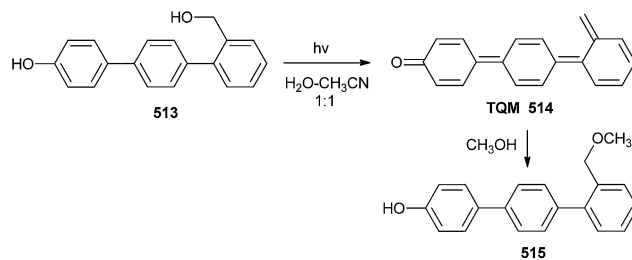


Scheme 110 Tautomerization in quinone methide.

There was no pH effect on the photosolvolytic quantum yield of the hydroxyterphenyls **513** in the pH 4–12 region, so the most probable mechanism for photosolvolytic is the formation of excited state phenolate followed by dehydroxylation to give terphenyl quinone methides (TQM, **514**), which after reaction with methanol gives compound **515** (Scheme 112).<sup>107a</sup>

Compound **516** with competing photosolvolytic reaction generated compound **517** by the ESIPT process, with or without water.<sup>108</sup> At higher water contents, an intermediate **518** (with one or more water molecules) underwent the loss of hydroxide ions from the benzylic position with the assistance of the hydronium ion to generate quinone methide **519**, and finally over all solvolysis (attack by  $\text{CH}_3\text{OH}$  at the terminal quinone methide position) gave compound **520** (Scheme 113).

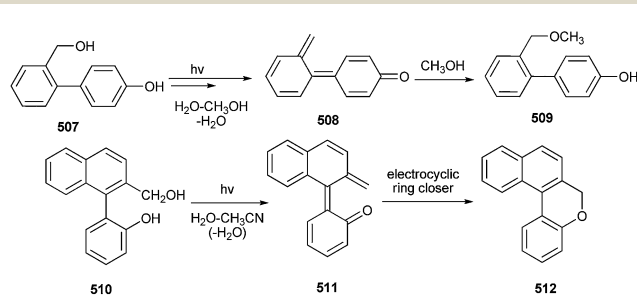
The compound 9-(2'-hydroxyphenyl) anthracene **521** undergoes proficient photoaddition of water and alcohols at the 9- and 10-positions of the anthracene moiety to give isolable



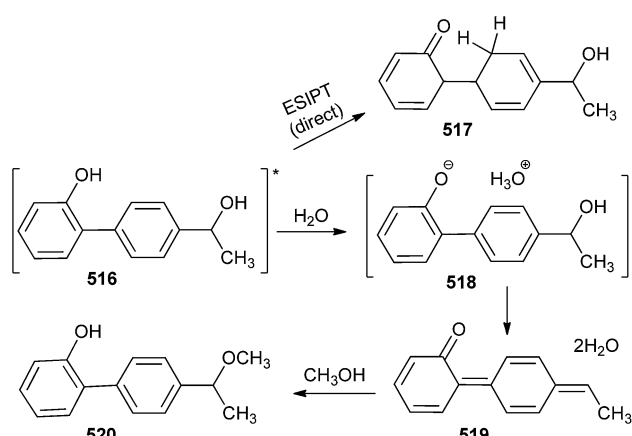
Scheme 112 Reaction of methanol with terphenyl quinone methide 514.

triphenylmethanol or triphenylmethyl ether type of products.<sup>21</sup> The reaction is supposed to ensue *via* water-mediated formal excited state an intramolecular proton transfer (ESIPT) from the phenolic OH to the 10-position of the anthracene ring, generating an *o*-QM intermediate that is observable by nanosecond laser flash photolysis, and is trappable with nucleophiles. Irradiation in deuterated solvents led to incorporation of one deuterium atom at the methylene position in the photoaddition product, and partial deuterium exchange of the 10-position of recovered starting material, which is reliable with the proposed formal excited state proton transfer mechanism (Scheme 114). The deuterium exchange and the photoaddition have got maximum quantum efficiency in 5 M water (in  $\text{CH}_3\text{CN}$  or  $\text{CH}_3\text{OH}$ ), and no reaction was observed in the absence of a hydroxylic solvent, thus representing the sensitivity of this type of ESIPT to solvent composition. Once formed, QM **522** is transformed to **523** (hydration product) or returns to **521** *via* enolization. These two reaction pathways from **522** are not really astonishing apart from the isolation of the stable anthracene hydrates and alcohol adducts (Scheme 114).

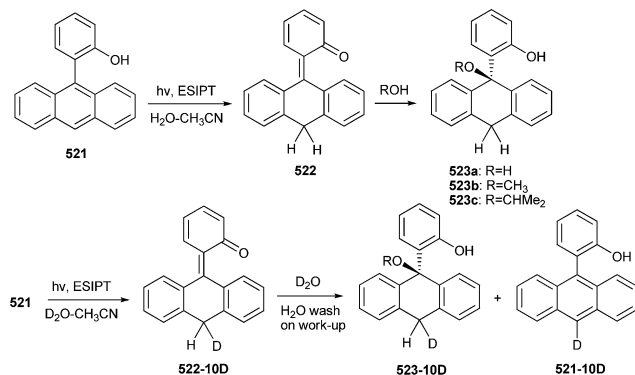
In general, caged carbonyl compounds<sup>109</sup> are prepared by their acetalization with (2,5-dimethoxyphenyl)ethylene glycol followed by oxidative demethylation to produce the corresponding (1,3-dioxolane-4-yl)-1,4-benzoquinones. (2,5-Dihydroxyphenyl) ethylene glycol acetals of aldehydes and ketones **524a–e** upon irradiation (at 300 nm) resulted in their efficient



Scheme 111 Photochemical synthesis of compounds 509 and 512.



Scheme 113 Photosolvolytic reaction of quinone methide 519.



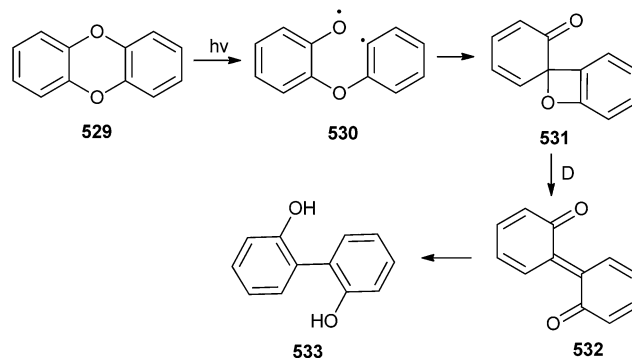
**Scheme 114** Photoaddition of hydroxylc solvents at 10-position of the anthracene.

cleavage and in the regeneration of the carbonyl compound. This proceeds *via* photoinduced transfer of the phenolic proton to the dioxolane oxygen in the 3-position accompanied by the C–O bond cleavage and the formation of an intermediate *o*-QM 525. *o*-QM is very reactive and could undergo rapid hydration or tautomerization to form corresponding unstable hemiacetals 526 and/or 527. The hydrolysis of 526 and 527 liberates the carbonyl compound 528 (Scheme 115).

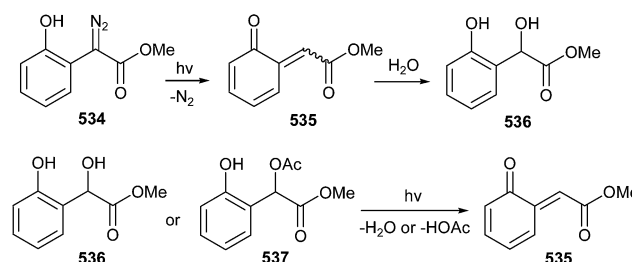
The dibenz[1,4]dioxins 529 underwent a photochemical aryl-ether bond homolysis to generate reactive 2-spiro-6-cyclohexa-2,4-dienone 531 and subsequent biphenylquinone intermediates.<sup>110</sup> Under steady-state irradiation, the 2,2'-biphenyl-quinones 532 undergo an excited state hydrogen abstraction from the organic solvent to give the corresponding 2,2-dihydrobiphenyls 533 (Scheme 116).

The flash photolysis of methyl 2-hydroxyphenyldiazoacetate 534 in dilute aqueous perchloric acid solution and acetic acid and biphosphosphate ion buffers generated a transient species that was identified as *o*-quinone- $\alpha$ -carbomethoxymethide 535 (Scheme 117).<sup>111</sup> This structural assignment is based on the solvent isotope effects, the form of buffer catalysis, UV absorption maxima, and the identity of decay rate constants with those determined for the transient, obtained by flash photolysis of other more conventional quinone methide precursors such as the benzyl alcohol methyl 2-hydroxy mandelate 536 and its acetate, 2-acetoxy-2-hydroxyphenylacetate 537.

New (2-adamantyl)naphthol derivatives 536–540, quinone methide precursors (QMP, Scheme 118) were synthesized and

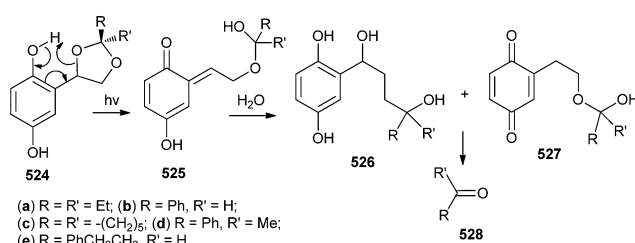


**Scheme 116** Photochemical aryl-ether bond homolysis of dibenz[1,4]dioxin.

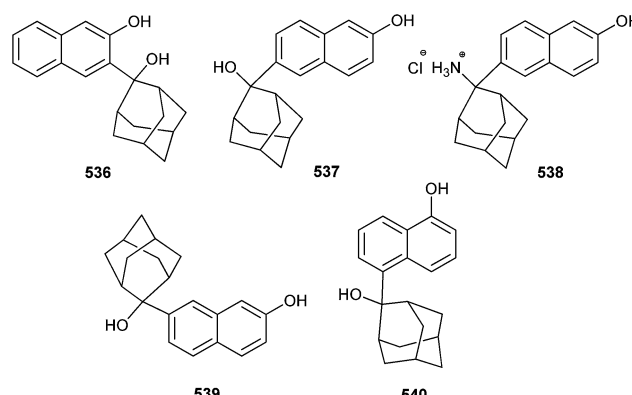


**Scheme 117** Photolysis of methyl 2-hydroxyphenyldiazoacetate.

their photochemical reactivity was investigated by preparative photolyses, fluorescence spectroscopy, and laser flash photolysis (LFP). All derivatives undergo photosolvolytic *via* QM intermediates. Presence of adamantly moiety results in different reactivity pattern compared to the non-substituted structure. They also investigated the anti-proliferative activity of the QMPs on three human cancer cell lines: HCT 116 (colon), MCF-7 (breast), and H 460 (lung). Exposure of cells treated with 5 to 300 nm of irradiation led to enhanced anti-proliferative effect on MCF-7 cell line, classifying 5 (or QM5) as a potential lead for further anti-proliferative studies.<sup>112</sup>



**Scheme 115** Regeneration of the carbonyl compound by irradiation of ethylene glycol acetals.



**Scheme 118** Quinone methide precursors of (2-adamantyl)naphthol derivatives.

## 4. Concluding remarks

In this review, we present the power and diversity of applications of *ortho*-quinone methides (*o*-QMs), which have become powerful, fascinating, and highly efficient intermediates in organic synthesis. Recent advances toward the generation, reactivity and application of *o*-QMs in organic synthesis offer a bright future for the development of novel methodologies for the synthesis of natural and man-made compounds. The cases cited in this review have been selected to highlight the most promising applications of *o*-QMs in organic synthesis. It can be seen that many well-established different methodologies were successfully applied to *o*-QMs by worldwide laboratories to more environmentally benign approaches. This area is clearly expanding in several aspects and will reveal spectacular applications in the near future, ranging from organic synthesis, material chemistry, fine chemicals, and pharmaceuticals to the synthesis of natural products. Definitely, much more remains to be done in this field, and in the next few years, we will see many new, exciting findings in *o*-QMs chemistry. Moreover, it will lead to the serendipitous discovery of many more new reactions, for as much as we may know, chemistry always has new and intriguing surprises in store. Therefore, we sincerely hope that this overview will be of interest for the synthetic community as well as for the general readers. Despite the flurry of recent interest in this species, it is unlikely that we have seen a peak, and it is probable that in future years *o*-QMs will be viewed in the same light as radicals, carbenes, benzynes or similar reactive intermediates.

## Acknowledgements

We sincerely thank all co-workers and collaborators whose names appear in the related references for their great contribution to the project. The financial support from the Science and Engineering Research Board (SERB) and the Council of Scientific and Industrial Research (CSIR), New Delhi is gratefully acknowledged. A.N., S.C. and N.A. thank University Grants Commission, New Delhi for fellowship.

## Notes and references

- 1 For reviews see: (a) R. W. V. D. Water and T. R. R. Pettus, *Tetrahedron*, 2002, **58**, 5367–5405; (b) H. Amouri and J. L. Bras, *Acc. Chem. Res.*, 2002, **35**, 501–510; (c) S. B. Ferreira, F. D. C. da Silva, A. C. Pinto, D. T. G. Gonzaga and V. F. Ferreira, *J. Heterocycl. Chem.*, 2009, **46**, 1080–1097.
- 2 (a) R. Li, X. Wang, Z. Wei, C. Wu and F. Shi, *Org. Lett.*, 2013, **15**, 4366–4369; (b) A. Kumar, M. Kumar and M. K. Gupta, *Green Chem.*, 2012, **14**, 2677–2681.
- 3 N. J. Willis and C. D. Bray, *Chem.-Eur. J.*, 2012, **18**, 9160–9173.
- 4 (a) *Quinone Methides*, ed. S. E. Rokita, Wiley, Hoboken, NJ, 2009; (b) H. Wang and S. E. Rokita, *Angew. Chem., Int. Ed.*, 2010, **49**, 5957–5960.
- 5 E. Modica, R. Zanaletti, M. Freccero and M. Mella, *J. Org. Chem.*, 2001, **66**, 41–52.
- 6 D. Zhang, M. Ogan, R. Gedamke, V. Roongta, R. Dai, M. Zhu, J. K. Rinehart, L. Klunk and J. Mitroka, *Drug Metab. Dispos.*, 2003, **7**, 837–845.
- 7 (a) S. E. Rokita, J. Yang, P. Pande and W. A. Greenberg, *J. Org. Chem.*, 1997, **62**, 3010–3012; (b) W. F. Veldhuyzen, A. J. Shallop, R. A. Jones and S. E. Rokita, *J. Am. Chem. Soc.*, 2001, **123**, 11126–11132.
- 8 (a) P. Pande, J. Shearer, J. Yang, W. A. Greenberg and S. E. Rokita, *J. Am. Chem. Soc.*, 1999, **121**, 6773–6779; (b) P. Wang, R. Liu, X. Wu, H. Ma, X. Cao, P. Zhou, J. Zhang, X. Weng, X. L. Zhang, X. Zhou and L. Weng, *J. Am. Chem. Soc.*, 2003, **125**, 1116–1117; (c) D. Verga, S. N. Richter, M. Palumbo, R. Gandolfi and M. Freccero, *Org. Biomol. Chem.*, 2007, **5**, 233–235; (d) S. E. Wolkenberg and D. L. Boger, *Chem. Rev.*, 2002, **102**, 2477–2495.
- 9 T. H. Koch, B. L. Barthel, B. T. Kalet, D. L. Rudnicki, G. C. Post and D. J. Burkhardt, *Top. Curr. Chem.*, 2008, **283**, 141–170.
- 10 (a) S. R. Angle and W. Yang, *J. Am. Chem. Soc.*, 1990, **112**, 4524–4528; (b) G. Gaudiano, M. Frigerio, P. Bravo and T. H. Koch, *J. Am. Chem. Soc.*, 1990, **112**, 6704–6709; (c) G. Gaudiano and T. H. Koch, *Chem. Res. Toxicol.*, 1991, **4**, 2–16; (d) S. R. Angle and W. Yang, *J. Org. Chem.*, 1992, **57**, 1092–1097; (e) S. R. Angle, J. D. Rainer and C. Woytowicz, *J. Org. Chem.*, 1997, **62**, 5884–5892.
- 11 P. Wang, Y. Song, L. Zhang, H. He and X. Zhou, *Curr. Med. Chem.*, 2005, **12**, 2893–2913.
- 12 R. Rodriguez, R. M. Adlington, J. E. Moses, A. Cowley and J. E. Baldwin, *Org. Lett.*, 2004, **6**, 3617–3619.
- 13 C. D. Bray, *Org. Biomol. Chem.*, 2008, **6**, 2815–2819.
- 14 A. F. Barrero, J. F. Q. del Moral, M. M. Herrador, P. Arteaga, M. Cortes, J. Benites and A. Rosellon, *Tetrahedron*, 2006, **62**, 6012–6017.
- 15 K. Wojciechowski and K. Dolatowska, *Tetrahedron*, 2005, **61**, 8419–8422.
- 16 H. Sugimoto, S. Nakamura and T. Ohwada, *J. Org. Chem.*, 2007, **72**, 10088–10095.
- 17 J. Delgado, A. Espinos, M. C. Jimenez and M. A. Miranda, *Chem. Commun.*, 2002, 2636–2637.
- 18 M. K. Boyd and G. M. Zopp, *Annu. Rep. Prog. Chem., Sect. B: Org. Chem.*, 2002, **98**, 543–579.
- 19 (a) Y. Chiang, A. J. Kresge and Y. Zhu, *J. Am. Chem. Soc.*, 2002, **124**, 717–722; (b) Y. Chiang, A. J. Kresge and Y. Zhu, *J. Am. Chem. Soc.*, 2001, **123**, 8089–8094.
- 20 M. Lukeman and P. Wan, *J. Am. Chem. Soc.*, 2002, **124**, 9458–9464.
- 21 M. Flegel, M. Lukeman, L. Huck and P. Wan, *J. Am. Chem. Soc.*, 2004, **126**, 7890–7897.
- 22 Y. Chiang, A. J. Kresge, O. Sadovski and H.-Q. Zhan, *J. Org. Chem.*, 2005, **70**, 1643–1646.
- 23 J. Matsumoto, M. Ishizu, R. Kawano, D. Hesaka, T. Shiragami, Y. Hayashi, T. Yamashita and M. Yasuda, *Tetrahedron*, 2005, **61**, 5735–5740.
- 24 (a) S. Arumugam and V. V. Popik, *J. Am. Chem. Soc.*, 2009, **131**, 11892–11899; (b) A. Kulikov, S. Arumugam and

V. V. Popik, *J. Org. Chem.*, 2008, **73**, 7611–7615; (c) S. Arumugam and V. V. Popik, *J. Org. Chem.*, 2010, **75**, 7338–7346.

25 N. Basaric, I. Zabecic, K. M. Majerski and P. Wan, *J. Org. Chem.*, 2010, **75**, 102–116.

26 S. N. Richter, S. Maggi, S. C. Mels, M. Palumbo and M. Freccero, *J. Am. Chem. Soc.*, 2004, **126**, 13973–13979.

27 D. Skalamera, K. M. Majerski, I. M. Kleiner, M. Kralj, P. Wan and N. Basaric, *J. Org. Chem.*, 2014, **79**, 4390–4397.

28 F. Doria, C. Percivalle and M. Freccero, *J. Org. Chem.*, 2012, **77**, 3615–3619.

29 M. J. Adler and S. W. Baldwin, *Tetrahedron Lett.*, 2009, **50**, 5075–5079.

30 (a) K. Nakatani, N. Higashida and I. Saito, *Tetrahedron Lett.*, 1997, **38**, 5005–5008; (b) K. Chiba, T. Hirano, Y. Kitano and M. Tada, *Chem. Commun.*, 1999, 691–692.

31 P. Batsomboon, W. Phakhodee, S. Ruchirawat and P. Ploypradith, *J. Org. Chem.*, 2009, **74**, 4009–4012.

32 Y. Sawama, Y. Shishido, T. Yanase, K. Kawamoto, R. Goto, Y. Monguchi, Y. Kita and H. Sajiki, *Angew. Chem. Int. Ed.*, 2013, **52**, 1515–1519.

33 O. O. Fadeyi, R. N. Daniels, S. M. DeGuire and C. W. Lindsley, *Tetrahedron Lett.*, 2009, **50**, 3084–3087.

34 P.-J. J. Huang, T. S. Cameron and A. Jha, *Tetrahedron Lett.*, 2009, **50**, 51–54.

35 Y. R. Lee, Y. M. Kim and S. H. Kim, *Tetrahedron*, 2009, **65**, 101–108.

36 H. Yoshida, Y. Ito and J. Ohshita, *Chem. Commun.*, 2011, **47**, 8512–8514.

37 D. Liao, H. Li and X. Lei, *Org. Lett.*, 2012, **14**, 18–21.

38 S. B. Bharate and I. P. Singh, *Tetrahedron Lett.*, 2006, **47**, 7021–7024.

39 (a) A. L. Lawrence, R. M. Adlington, J. E. Baldwin, V. Lee, J. A. Kershaw and A. L. Thompson, *Org. Lett.*, 2010, **12**, 1676–1679; (b) X.-L. Yang, K.-L. Hsieh and J.-K. Liu, *Org. Lett.*, 2007, **9**, 5135–5138.

40 C. Selenski and T. R. R. Pettus, *J. Org. Chem.*, 2004, **69**, 9196–9203.

41 (a) R. V. De Water, D. Magdziak, J. Chau and T. R. R. J. Pettus, *J. Am. Chem. Soc.*, 2000, **122**, 6502–6503; (b) A. Arduini, A. Bosi, A. Pochini and R. Ungaro, *Tetrahedron*, 1985, **41**, 3095–3103; (c) C. Selenski, L. Mejorado and T. R. R. Pettus, *Synlett*, 2004, 1101–1103.

42 S. B. Bharate, S. I. Khan, B. L. Tekwani, M. Jacob, I. A. Khan and I. P. Singh, *Bioorg. Med. Chem.*, 2008, **16**, 1328–1336.

43 S. B. Bharate, K. K. Bhutani, S. I. Khan, B. L. Tekwani, M. R. Jacob, I. A. Khan and I. P. Singh, *Bioorg. Med. Chem.*, 2006, **14**, 1750–1760.

44 L. W. Schenck, K. Kuna, W. Frank, A. Albert, C. Asche and U. Kucklaender, *Bioorg. Med. Chem.*, 2006, **14**, 3599–3614.

45 Y. Chen and M. G. Steinmetz, *J. Org. Chem.*, 2006, **71**, 6053–6060.

46 A. F. Barrero, J. F. Q. del Moral, M. M. Herrador, P. Arteaga, M. Cortes, J. Benites and A. Rosellon, *Tetrahedron*, 2006, **62**, 6012–6017.

47 K. Tchabanenko, M. G. O. Taylor, R. M. Adlington and J. E. Baldwin, *Tetrahedron Lett.*, 2006, **47**, 39–41.

48 C. C. Lindsey and T. R. R. Pettus, *Tetrahedron Lett.*, 2006, **47**, 201–204.

49 (a) F. Liebner, P. Schmid, C. Adelwohrer and T. Rosenau, *Tetrahedron*, 2007, **63**, 11817–11821; (b) T. Rosenau, *Encyclopedia of Vitamin E*, ed. V. R. Preedy and R. R. Watson, CABI: Oxford, Cambridge, 2007, pp. 21–44 and 69–96.

50 E. Alden-Danforth, M. T. Scerba and T. Lectka, *Org. Lett.*, 2008, **10**, 4951–4953.

51 M. A. Marsini, Y. Huang, C. C. Lindsey, K.-L. Wu and T. R. R. Pettus, *Org. Lett.*, 2008, **10**, 1477–1480.

52 S. J. Gharpure, A. M. Sathianarayanan and P. Jonnalagadda, *Tetrahedron Lett.*, 2008, **49**, 2974–2978.

53 T. B. Samarakoon, M. Y. Hur, R. D. Kurtz and P. R. Hanson, *Org. Lett.*, 2010, **12**, 2182–2185.

54 J. C. Green and T. R. R. Pettus, *J. Am. Chem. Soc.*, 2011, **133**, 1603–1608.

55 T. Rosenau, C. Adelwohrer, E. Kloser, K. Mereiter and T. Netscher, *Tetrahedron*, 2006, **62**, 1772–1776.

56 H. M. Fales, H. A. Lloyd, J. A. Ferretti, J. V. Silverton, D. G. Davis and H. J. Kon, *J. Chem. Soc., Perkin Trans. 2*, 1990, 1005–1010.

57 (a) G. C. Nandi, S. Samai, R. Kumar and M. S. Singh, *Tetrahedron*, 2009, **65**, 7129–7134; (b) S. Samai, G. C. Nandi and M. S. Singh, *Tetrahedron*, 2012, **68**, 1247–1252; (c) R. Kumar, G. C. Nandi, R. K. Verma and M. S. Singh, *Tetrahedron Lett.*, 2010, **51**, 442–445.

58 B. Datta and M. A. Pasha, *Ultrason. Sonochem.*, 2011, **18**, 624–628.

59 G. C. Nandi, S. Samai, R. Kumar and M. S. Singh, *Tetrahedron Lett.*, 2009, **50**, 7220–7222.

60 R. R. Nagawade and D. B. Shinde, *Mendeleev Commun.*, 2007, **17**, 299–300.

61 M. M. Khodaei, A. R. Khosropour and H. Moghanian, *Synlett*, 2006, 916–920.

62 M. Hong, C. Cai and W. B. Yi, *Chin. Chem. Lett.*, 2011, **22**, 322–325.

63 H. R. Shaterian and H. Yarahmadi, *ARKIVOC*, 2008, **ii**, 105–114.

64 A. Dorehgiraei, H. Khabazzadeh and K. Saidi, *ARKIVOC*, 2009, **vii**, 303–310.

65 (a) A. Kumar, M. S. Rao and V. K. Rao, *Aust. J. Chem.*, 2010, **63**, 1538–1540; (b) A. Hosseini and H. R. Shaterian, *Phosphorus, Sulfur Silicon Relat. Elem.*, 2012, **187**, 1056–1063; (c) A. Shaabani, A. Rahmati and E. Farhangi, *Tetrahedron Lett.*, 2007, **48**, 7291–7294.

66 V. A. Osyanin, D. V. Osipov and Y. N. Klimochkin, *J. Org. Chem.*, 2013, **78**, 5505–5520.

67 F. Mazzini, T. Netscher and P. Salvadoria, *Tetrahedron*, 2005, **61**, 813–817.

68 C. Adelwohrer, T. Rosenau, W. H. Binder and P. Kosma, *Tetrahedron*, 2003, **59**, 3231–3235.

69 M.-W. Chen, L.-L. Cao, Z.-S. Ye, G.-F. Jiang and Y.-G. Zhou, *Chem. Commun.*, 2013, **49**, 1660–1662.

70 Y. Luan and S. E. Schaus, *J. Am. Chem. Soc.*, 2012, **134**, 19965–19968.

71 A. Kumar, M. Kumar, M. K. Gupta and L. P. Gupta, *RSC Adv.*, 2012, **2**, 8277–8280.

72 C. Percivalle, A. La Rosa, D. Verga, F. Doria, M. Mella, M. Palumbo, M. Di Antonio and M. Freccero, *J. Org. Chem.*, 2011, **76**, 3096–3106.

73 M. Nadai, F. Doria, M. Di Antonio, G. Sattin, L. Germani, C. Percivalle, M. Palumbo, S. N. Richter and M. Freccero, *Biochimie*, 2011, **93**, 1328–1340.

74 E. E. Weinert, K. N. Frankenfield and S. E. Rokita, *Chem. Res. Toxicol.*, 2005, **18**, 1364–1370.

75 E. Modica, R. Zanaletti, M. Freccero and M. Mella, *J. Org. Chem.*, 2001, **66**, 41–52.

76 E. E. Weinert, R. Dondi, S. Colloredo-Melz, K. N. Frankenfield, C. H. Mitchell, M. Freccero and S. E. Rokita, *J. Am. Chem. Soc.*, 2006, **128**, 11940–11947.

77 E. E. Weinert, K. N. Frankenfield and S. E. Rokita, *Chem. Res. Toxicol.*, 2005, **18**, 1364–1370.

78 Q. Zhou and S. E. Rokita, *Proc. Natl. Acad. Sci. U. S. A.*, 2003, **100**, 15452–15457.

79 M. P. McCrane, E. E. Weinert, Y. Lin, E. P. Mazzola, Y.-F. Lam, P. F. Scholl and S. E. Rokita, *Org. Lett.*, 2011, **13**, 1186–1189.

80 Y. Chiang and A. J. Kresge, *Org. Biomol. Chem.*, 2004, **2**, 1090–1092.

81 Y. Du, X. Weng, J. Huang, D. Zhang, H. Ma, D. Chen, X. Zhou and J.-F. Constant, *Bioorg. Med. Chem.*, 2010, **18**, 4149–4153.

82 J. Zhang, X. Wu, X. Cao, F. Yang, J. Wang, X. Zhou and X.-L. Zhang, *Bioorg. Med. Chem. Lett.*, 2003, **13**, 1097–1100.

83 Y. Song, P. Wang, J. Wu, X. Zhou, X.-L. Zhang, L. Weng, X. Cao and F. Liang, *Bioorg. Med. Chem. Lett.*, 2006, **16**, 1660–1664.

84 Q. Zhou, T. Xu and J. B. Mangrum, *Chem. Res. Toxicol.*, 2007, **20**, 1069–1074.

85 M. Di Antonio, F. Doria, S. N. Richter, C. Bertipaglia, M. Mella, C. Sissi, M. Palumbo and M. Freccero, *J. Am. Chem. Soc.*, 2009, **131**, 13132–13141.

86 F. Doria, S. N. Richter, M. Nadai, S. Colloredo-Mels, M. Mella, M. Palumbo and M. Freccero, *J. Med. Chem.*, 2007, **50**, 6570–6579.

87 M. Freccero, R. Gandolfi and M. Sarzi-Amade, *J. Org. Chem.*, 2003, **68**, 6411–6423.

88 T. A. Wenderski, S. Huang and T. R. R. Pettus, *J. Org. Chem.*, 2009, **74**, 4104–4109.

89 T. Okugaki, M. Kasuno, K. Maeda and S. Kihara, *J. Electroanal. Chem.*, 2010, **639**, 67–76.

90 K. A. Korthals and W. D. Wulff, *J. Am. Chem. Soc.*, 2008, **130**, 2898–2899.

91 A. V. Vorogushin, W. D. Wulff and H.-J. Hansen, *Tetrahedron*, 2008, **64**, 949–968.

92 K. H. Jensen, J. D. Webb and M. S. Sigman, *J. Am. Chem. Soc.*, 2010, **132**, 17471–17482.

93 K. M. Gligorich, Y. Iwai, S. A. Cummings and M. S. Sigman, *Tetrahedron*, 2009, **65**, 5074–5083.

94 S. M. Stokes Jr, F. Ding, P. L. Smith, J. M. Keane, M. E. Kopach, R. Jervis, M. Sabat and W. D. Harman, *Organometallics*, 2003, **22**, 4170–4171.

95 S. Radomkit, P. Sarnpitak, J. Tummatorn, P. Batsomboon, S. Ruchirawat and P. Ploypradith, *Tetrahedron*, 2011, **67**, 3904–3914.

96 D. A. Lev, D. B. Grotjahn and H. Amouri, *Organometallics*, 2005, **24**, 4232–4240.

97 J. C. J. M. D. S. Menezes, A. T. P. C. Gomes, A. M. S. Silva, M. A. F. Faustino, M. G. P. M. S. Neves, A. C. Tomé, F. C. da Silva, V. F. Ferreira and J. A. S. Cavaleiro, *Synlett*, 2011, 1841–1844.

98 S.-T. Huang, K.-N. Ting and K.-L. Wang, *Anal. Chim. Acta*, 2008, **620**, 120–126.

99 G. da Silva and J. W. Bozzelli, *J. Phys. Chem. A*, 2007, **111**, 7987–7994.

100 A. Koll, A. Karpfen and P. Wolschann, *J. Mol. Struct.*, 2006, **790**, 55–64.

101 S. Takekuma, M. Tamura, T. Minematsu and H. Takekuma, *Tetrahedron*, 2007, **63**, 12058–12070.

102 G. Vincent, J. W. Lane and R. M. Williams, *Tetrahedron Lett.*, 2007, **48**, 3719–3722.

103 H. Jacobs, W. J. F. van der Vijgh, G. H. Koek, G. J. J. Draaisma, M. Moalin, G. P. F. van Strijdonck, A. Bast and G. R. M. M. Haenen, *Free Radical Biol. Med.*, 2009, **46**, 1567–1573.

104 A. Pezzella, L. Panzella, O. Crescenzi, A. Napolitano, S. Navaratman, R. Edge, E. J. Land, V. Barone and M. Ischia, *J. Am. Chem. Soc.*, 2006, **128**, 15490–15498.

105 J. K. Harper, A. M. Arif, E. J. Ford, G. A. Strobel, J. A. Porco Jr, D. P. Tomer, K. L. O'Neill, E. M. Heidere and D. M. Granta, *Tetrahedron*, 2003, **59**, 2471–2476.

106 U. S. M. Maharoof and G. A. Sulikowski, *Tetrahedron Lett.*, 2003, **44**, 9021–9023.

107 (a) M. Xu, C. Z. Chen and P. Wan, *J. Photochem. Photobiol. A*, 2008, **198**, 26–33; (b) C.-G. Huang, K. A. Beveridge and P. Wan, *J. Am. Chem. Soc.*, 1991, **113**, 7676–7684; (c) Y. Shi and P. Wan, *J. Chem. Soc., Chem. Commun.*, 1995, 1217–1218; (d) M. Lukeman and P. Wan, *J. Am. Chem. Soc.*, 2003, **125**, 1164–1165.

108 N. B. Aein and P. Wan, *J. Photochem. Photobiol. A*, 2009, **208**, 42–49.

109 A. P. Kostikov, N. Malashikhina and V. V. Popik, *J. Org. Chem.*, 2009, **74**, 1802–1804.

110 S. Rayne, R. Sasaki and P. Wan, *Photochem. Photobiol. Sci.*, 2005, **4**, 876–886.

111 Y. Chiang, A. J. Kresge and Y. Zhu, *Phys. Chem. Chem. Phys.*, 2003, **5**, 1039–1042.

112 J. Veljkovic, L. Uzelac, K. Molcanov, K. M. Majerski, M. Kralj, P. Wan and N. Basaric, *J. Org. Chem.*, 2012, **77**, 4596–4610.